J Physiol 589.24 (2011) pp 5965–5986

The Journal of Physiology

Control of hypothalamic–pituitary–adrenal stress axis activity by the intermediate conductance calcium-activated potassium channel, SK4

Zhi Liang[1], Lie Chen[1], Heather McClafferty[1], Robert Lukowski[2], Duncan MacGregor[1], Jonathan T. King[3], Sandra Rizzi[4], Matthias Sausbier[2], David P. McCobb[3], Hans-Guenther Knaus[4], Peter Ruth[2] and Michael J. Shipston[1]

[1] *Centre for Integrative Physiology, Hugh Robson Building, College of Medicine and Veterinary Medicine, University of Edinburgh, Edinburgh EH89XD, Scotland, UK*

[2] *Pharmacology and Toxicology, Institute of Pharmacy, University of Tübingen, 72076 Tübingen, Germany*

[3] *Neurobiology and Behaviour, Cornell University, Ithaca, NY, USA*

[4] *Division of Molecular and Cellular Pharmacology, Medical University Innsbruck, Innsbruck A-6020, Austria*

Non-technical summary Our ability to respond to stress is critically dependent upon the release of the stress hormone adrenocorticotrophic hormone (ACTH) from corticotroph cells of the anterior pituitary gland. ACTH release is controlled by the electrical properties of corticotrophs that are determined by the movement of ions through channel pores in the plasma membrane. We show that a calcium-activated potassium ion channel called SK4 is expressed in corticotrophs and regulates ACTH release. We provide evidence of how SK4 channels control corticotroph function, which is essential for understanding homeostasis and for treating stress-related disorders.

Abstract The anterior pituitary corticotroph is a major control point for the regulation of the hypothalamic–pituitary–adrenal (HPA) axis and the neuroendocrine response to stress. Although corticotrophs are known to be electrically excitable, ion channels controlling the electrical properties of corticotrophs are poorly understood. Here, we exploited a lentiviral transduction system to allow the unequivocal identification of live murine corticotrophs in culture. We demonstrate that corticotrophs display highly heterogeneous spontaneous action-potential firing patterns and their resting membrane potential is modulated by a background sodium conductance. Physiological concentrations of corticotrophin-releasing hormone (CRH) and arginine vasopressin (AVP) cause a depolarization of corticotrophs, leading to a sustained increase in action potential firing. A major component of the outward potassium conductance was mediated via intermediate conductance calcium-activated (SK4) potassium channels. Inhibition of SK4 channels with TRAM-34 resulted in an increase in corticotroph excitability and exaggerated CRH/AVP-stimulated ACTH secretion *in vitro*. In accordance with a physiological role for SK4 channels *in vivo*, restraint stress-induced plasma ACTH and corticosterone concentrations were significantly enhanced in gene-targeted mice lacking SK4 channels ($Kcnn4^{-/-}$). In addition, $Kcnn4^{-/-}$ mutant mice displayed enhanced hypothalamic c-fos and nur77 mRNA expression following restraint, suggesting increased neuronal activation. Thus, stress hyperresponsiveness observed in $Kcnn4^{-/-}$ mice results from enhanced secretagogue-induced ACTH output from anterior pituitary corticotrophs and may also involve increased hypothalamic drive, thereby suggesting an important role for SK4 channels in HPA axis function.

DOI: 10.1113/jphysiol.2011.219378

(Received 24 August 2011; accepted after revision 28 October 2011; first published online 31 October 2011)
Corresponding author M. J. Shipston: Centre for Integrative Physiology, Hugh Robson Building, University of Edinburgh, Edinburgh, Scotland, UK. Email: mike.shipston@ed.ac.uk

Abbreviations ACTH, adrenocorticotrophin hormone; AVP, arginine vasopressin; BK, large conductance calcium- and voltage-activated potassium channel; c-*fos* cellular FBJ murine osteosarcoma viral oncogene homologue; CRH, corticotrophin releasing hormone; eYFP, enhanced yellow fluorescent protein; GR, glucocorticoid receptor; HPA, hypothalamic–pituitary–adrenal; MR, mineralocorticoid receptor; *nurr*77, nerve growth factor inducible gene-B; POMC, proopiomelanocortin; PVN, paraventricular nucleus of the hypothalamus.

Introduction

The ability to respond to external stressors as well as perturbations of the internal environment is essential to the long term survival and healthy ageing of organisms. The hypothalamic–pituitary–adrenal axis (HPA axis) represents the major neuroendocrine response to stress, by coordinating appropriate responses to sensory input. Stressors ultimately activate hypothalamic neuroendocrine neurones in the paraventricular nucleus, releasing corticotrophin releasing hormone (CRH) and arginine vasopressin (AVP) into the portal circulation. CRH and AVP act on the anterior pituitary corticotrophs to stimulate release of adrenocorticotrophin hormone (ACTH). ACTH is released into the systemic circulation to control release of the powerful glucocorticoid hormones (cortisol in man, corticosterone in rodents) from the adrenal gland. Glucocorticoids in turn feedback at multiple levels of the HPA axis to terminate the stress response. Acute activation of the HPA axis is required for stress adaptation, but prolonged and/or excessive levels of stress hormones, in particular glucocorticoids, may predispose to major metabolic, immune, cardiovascular and affective disorders (Antoni, 1986; Dallman *et al.* 1987; Sapolsky *et al.* 2000; McEwen & Wingfield, 2003).

The anterior pituitary corticotroph represents a major 'hub' in the control of the HPA axis function, integrating efferent signals from the brain with feedback control from circulating steroid hormones to coordinate ACTH release. Stimulatory (e.g. CRH and AVP) and inhibitory factors controlling ACTH output from pituitary corticotrophs are well characterised. Furthermore, it is now well established that anterior pituitary corticotrophs in many species are electrically excitable, as are other cells of the anterior pituitary gland (Stojilkovic *et al.* 2010). However, ion channels and mechanisms controlling corticotroph excitability and its coupling to calcium-dependent ACTH secretion in corticotrophs remain poorly understood (Kuryshev *et al.* 1997; Lee & Tse, 1997). Considerable insight has been gained from a variety of tumour models, including variants of the mouse anterior pituitary cell line AtT20 (Surprenant, 1982; Pennington *et al.* 1994; Shipston *et al.* 1996) and cells from human pituitary corticotroph tumours (Mollard *et al.* 1987; Takano *et al.* 1996). However, the extent to which ionic mechanisms in these models truly reflect corticotroph function remains unclear. In part, this is a result of the major challenge of unequivocally distinguishing live corticotrophs from the variety of different anterior pituitary cell populations.

To address these issues several previous identification/labelling approaches have been exploited, including: (i) biotinylated CRH peptides to label corticotrophs (Childs *et al.* 1987), (ii) purification of corticotrophs following volume expansion in response to high doses of CRH by centrifugal elutriation (Ritchie *et al.* 1996; Kuryshev *et al.* 1997), (iii) identification based on ACTH release detected by haemolytic plaque assay (Lee & Tse, 1997), and (iv) *post hoc* staining of fixed cells for ACTH immunoreactivity or responsiveness to CRH or AVP (Brunton *et al.* 2007). Finally, a recent study has exploited transgenic mice constitutively expressing green fluorescent protein (GFP) under the control of the proopiomelanocortin (POMC; the precursor for ACTH synthesis) promoter (Lee *et al.* 2011), although analysis of spontaneous activity was not studied. Such studies have implicated a number of different ion channels and mechanisms in controlling corticotroph electrical excitability. However, in most cases analysis was performed with supramaximal concentrations of CRH or AVP several orders of magnitude greater than those reported in the portal circulation (Gibbs & Vale, 1982; Sheward & Fink, 1991). The difficulty in routine identification of living corticotrophs has precluded the systematic analysis of the spontaneous electrical excitability of these cells in the absence of secretagogues.

In this report, we have applied a highly efficient and selective labelling approach using lentiviral mediated transduction of primary murine pituitary cells *in vitro* with a fluorescent (enhanced yellow fluorescent protein; eYFP) construct driven by a minimal POMC promoter. Using this approach, we have characterised the electrical properties of unstimulated and secretagogue-evoked murine corticotrophs in metabolically intact cells that are responsive to physiological concentrations of CRH and AVP. Importantly, our studies reveal a novel role for intermediate conductance calcium-activated potassium (SK4)

channels in corticotroph function, and reveal that mice genetically deficient for the channel display stress hyperresponsiveness.

Methods

Ethical approval

All experiments and tissue collection were performed between 08.00 h and 11.00 h and performed in accordance with accepted standards of humane animal care, UK Home Office requirements and the German legislation on protection of animals.

Lentiviral transduction of primary corticotrophs

Generation of POMC-eYFP lentiviral reporter. The POMC-eYFP lentiviral vector was constructed in the pLenti6/V5-D-TOPO vector. To facilitate subcloning steps we first generated new *Spe*I and *Sfu*I restriction sites flanking eYFP in the pEYFP-N1 vector. The subsequent *Spe*I and *Sfu*I restriction fragment containing eYFP from the mutant pEYFP-NI vector was then ligated into the pLenti6/V5-D-TOPO vector (Invitrogen) generating a construct (pLenti-CMV-eYFP) in which eYFP expression is driven by the CMV promoter. To generate a construct for expression restricted to POMC-expressing cells we amplified the rat minimal POMC promoter (−707 to +64 bp, a generous gift from Prof. Malcolm Low (University of Michigan Medical School); Hammer *et al.* 1990) from the pGEM TZ vector using forward and reverse primers (5′-TCATATCGATGCTTCCACTTCCCTCCACAG-3′ and 5′-CTGGACTAGTTGTTCAGTGGCCTCTCTTAG-3′) engineered to create *Cla*I and *Spe*I restriction sites, respectively. Amplicons were cloned into the pCRII-TOPO vector and the *Cla*I and *Spe*I fragment was ligated into the pLenti-CMV-eYFP construct to generate the pLenti-pomc-eYFP (available to academic laboratories on request) construct in which the minimal POMC promoter replaces the CMV promoter. To generate lentiviral particles the pLenti-CMV-eYFP or pLenti-pomc-eYFP plasmids were co-transfected with the psPAX2 packing plasmid (a generous gift from Prof. D. Trono, EPFL, Lausanne) and the pLP/VSVG envelope plasmid (Invitrogen) into HEK293FT cells. HEK293FT cells were seeded and cultured in a area correct, 75 cm^2 flask in growth medium 1 day before transient transfection at approximately 70% confluency. Before transfection, culture medium was replaced with fresh growth medium and the respective plenti6-POMC-eYFP, pLenti6-CMV-eYFP, psPAX2 and pLP/VSVG plasmids at a 4:3:2 ratio using ExGen 500 transfection reagent (Fermentas). After 24 h, the medium was replaced with 20 ml fresh growth medium, and the cells were harvested at 72 h post-transfection. The collected medium was spun at 4860 *g* for 15 min and the supernatant filtered through a 0.45 μm syringe filter (25 mmGD/X, Whatman) into a 15 ml Amicon Ultra-15 centrifugal filter device (Millipore, UK) and concentrated by spinning at 4860 *g* for 40–50 min. Lentivirus titre was determined using HEK293FT cells and defined as transduced Unit/ml lentiviral particles (TU ml^{-1}).

Transduction of primary murine anterior pituitary cells *in vitro*. Three to four female mice (mixed sv129/Bl6 background age range 2–5 months) were killed by cervical dislocation and the pituitaries were rapidly removed; the outer edges of the anterior lobes of the gland were removed to ensure no contamination from the intermediate lobe (which contains POMC-expressing melanotrophs). The anterior pituitary lobes were chopped with a single edged razor blade mounted on a McIlwain chopper (setting 0.7 mm) in both directions (rotated plate by 90 deg) and placed in Dulbecco's modified Eagle's medium (DMEM; Invitrogen) containing 25 mM Hepes, 0.25% trypsin and 10 μg ml^{-1} DNAse I, and incubated at 37°C for 20–25 min in a water bath. The tube was shaken every 5 min to achieve a complete and equal digestion. At the end of the digestion, tissue pieces settled to the bottom of the tube, and supernatant was aspirated. One millilitre of inhibitor solution (DMEM containing 0.5 mg ml^{-1} lima bean trypsin inhibitor, 100 kallikrein units aprotinin (200 × dilution of Sigma stock), 10 μg ml^{-1} DNAse I) was added and the tissue bits were triturated with a 1 ml Pipetman tip (Gilson) for approximately 40 times. The resulting suspension was filtered over a cell strainer with 70 μm nylon mesh (BD Biosciences (Franklin Lakes, NJ, USA)), diluted with an equal volume of culture medium (DMEM containing 25 mM Hepes, 5 μg ml^{-1} insulin, 50 μg ml^{-1} transferrin, 30 nM sodium selenite, 0.3% BSA (w/v), 4.2 μg ml^{-1} fibronectin and spun in a centrifuge at 100 *g* for 10 min. The pellet was triturated in 1 ml culture medium with 1% antibiotic/mycotic solution (Sigma), in order to disperse single cells. Cells from three to four anterior pituitaries were plated on 24 × 12 mm coverslips in a 6-well plate (4 coverslips per well) and incubated at 37°C in 5% CO_2. Pituitary cells were transduced 24 h after plating in antibiotic free culture medium. The culture medium was replaced with fresh medium 24 h post-transduction, culture medium was changed every 2 days, and fluorescent cells were typically used 48–72 h post-transduction.

Immunohistochemical co-labelling of transduced primary cells for ACTH. Primary mouse pituitary cells cultured on poly-D-lysine coated glass coverslips 2–4 days after lentiviral transduction were gently washed 3 times with phosphate buffered saline (PBS) containing 2 mM

$CaCl_2$ and 1 mM $MgCl_2$, and then fixed with 4% paraformaldehyde in PBS for 30 min at room temperature (RT). Following a quench step with 50 mM NH_4Cl for 10 min at RT, cells were washed, permeabilised with 0.3% (v/v) Triton X-100 in PBS (PBS-T) for 10 min and blocked with blocking solution (3% BSA in PBS-T) for 1 h at RT. Primary anti-ACTH antibody (1:500 in blocking solution, Sigma-Aldrich) was applied and incubated at 4°C overnight. Subsequently, cells were washed 3 times with PBS, rinsed in dH_2O and then incubated with Alexa-594 conjugated secondary antibody (1:1000) (Invitrogen, USA) in blocking solution for 1 h at RT. Cells were finally washed with PBS 3 times and mounted with Mowiol 4-88 mounting medium(Calbiochem, Damstadt, Germany)containing 1,4-diazabizyclo[2.2.2]octane (DABCO, Sigma) as antifade. Cells were imaged using a Zeiss LSM510 laser scanning confocal microscope equipped with a 63× (NA 1.4) oil immersion objective lens in multitracking mode.

Animals

Experiments with lentiviral-transduced cells were performed using virgin female mice (age range 2–5 months) on a mixed sv129/C57Bl6 background. In a limited number of experiments (predominantly to confirm aspects of pharmacological characterisation of potassium conductances) recordings were also performed using transgenic mice expressing GFP under control of the POMC promoter in a C57Bl6 background (a generous gift from Prof. J. Friedman (The Rockefeller University, NY, USA); Pinto *et al.* 2004). No significant differences in potassium conductances were observed between lentiviral transduced and transgenic corticotrophs (for example 1 μM clotrimazole inhibition of outward current was 38.4 ± 2.4 ($n = 5$) and 41.1 ± 3.8% ($n = 4$), respectively). Mice lacking the pore exon of the Kcnn4 channel α-subunit ($Kcnn4^{-/-}$), were generated previously (Sausbier *et al.* 2006). Wild-type (WT) and $Kcnn4^{-/-}$ mice on the hybrid SV129/C57BL6 background were used. Litter- and age-matched (F2 hybrid) adult female mice (age range 2–5 months, generated from F1 hybrid parents) were randomly assigned to each experimental condition. Mice were caged in groups of two to four under standard laboratory conditions (lights on at 07.00 h, lights off at 19.00 h, 21°C, with chow and tap water available *ad libitum*).

Electrophysiology

The perforated patch clamp configuration of the whole-cell recording technique was used for all whole cell current- and voltage-clamp recordings. Amphotericin was used at a final pipette concentration of 200 μg ml^{-1} with uncompensated access resistances between 15 and 30 MΩ, routinely achieved within 5–15 min of giga-ohm seal formation and stable for up to 1 h. The standard bath solution contained (in mM): 140 NaCl, 5 KCl, 2 $CaCl_2$, 0.1 $MgCl_2$, 10 Hepes and 10 glucose; pH 7.4 adjusted with NaOH, 300 mosmol l^{-1}. The standard pipette solution contained (in mM): 10 NaCl, 30 KCl, 60 K_2SO_4, 1 $MgCl_2$, 10 glucose, 10 Hepes and 50 sucrose; pH 7.2 adjusted with KOH, 290 mosmol l^{-1}. Cells were perfused using a gravity-driven perfusion system with flow rates <1.5 ml min^{-1} to minimise flow-induced artefacts.

Electrophysiological measurements in the inside-out configuration were made on corticotrophs from POMC-GFP transgenic mice. Experiments were conducted at 20–22°C. Patch electrodes (3–5 MΩ) were pulled from borosilicate glass (World Precision Instruments, Sarasota, FL, USA) and coated with silicone elastomer (Sylgard 184, Dow Corning). Data were collected using a List EPC-9 patch clamp amplifier, Bessel filtered at 10 kHz, and stored on a Power Macintosh G3 using Pulse 8.5 software (Heka Electronik, Lambrecht/Pfalz, Germany). Offline analysis was conducted with custom software written for Igor Pro (WaveMetrics, Inc., Lake Oswego, OR, USA). For inside-out patches, symmetrical K^+ solutions were used to eliminate potassium driving force and allow DC offset to be cancelled at 0 mV. The pipette and bath saline solutions contained (in mM): 160 KCl, 10 Hepes, 1 $MgCl_2$, 1 HEDTA, 0.188 $CaCl_2$, pH adjusted to 7.2 with KOH to obtain approximately 5 μM free [Ca^{2+}]. The free [Ca^{2+}] was calculated with MAXCHELATOR software (WEBMAXC v2.1; Bers *et al.* 1994). Zero-Ca^{2+} solution contained an additional 5 mM EGTA (Sigma). Paxilline (Sigma) was dissolved in 100% DMSO and stored at −20°C until the day of experiment, when it was diluted at least 1000× before use. The osmolarity of the saline solutions was measured by a dew point osmometer and adjusted to 300 mosmol l^{-1}.

Double immunofluorescence histochemistry of pituitary sections

Adult wild-type and $Kcnn4^{-/-}$ mice were deeply anaesthetized with 150 mg (kg body weight)$^{-1}$ thiopental (25 mg ml^{-1}; Sandoz) and immediately perfused via the left cardiac ventricle with PBS (pH 7.4) for 1 min, followed by ice-cold 4% paraformaldehyde in PBS for 10 min (approximately 45 ml) and PBS for 1 min. Pituitary glands were dissected and transferred into 20% sucrose in PBS for 18 h at 4°C. Thereafter, pituitary glands were snap frozen in prechilled (−70°C) isopentane (Merck) for 90 s and stored at −70°C. Sections of 10 μm were cut using

a cryostat and transferred onto polylysine coated slides and stored at −20°C for up to 8 weeks. Pituitary glands sections of 10 μm were washed twice in Tris-buffered saline (TBS; pH 7.4) for 5 min and permeabilized in 0.2% Triton X-100 in TBS (TBS-T) for 10 min. Slices were pre-incubated in 2% normal goat serum, 2% bovine serum albumin and 0.2% milk powder in TBS-T for 1 h at room temperature and incubated overnight with rabbit polyclonal anti-SK4 whole serum (Abcam Inc., Cambridge, MA, USA; no. 83740) diluted 1:1000 in 1% BSA in TBS-T. Sections were washed 10 min with TBS-T and incubated with mouse monoclonal anti-ACTH antibody, clone 02A3 (Dako, Carpenteria, CA, USA) diluted in 1% BSA in TBS-T 1:100 for 2 h at room temperature. Sections were washed with TBS-T for 30 min and incubated with secondary antibodies goat anti-rabbit Alexa-488 and goat anti-mouse Alexa-594 (both Invitrogen, nos A-11034 and A-11032) diluted 1:1000 in 2% BSA in TBS-T for 1 h at room temperature. Sections were washed with TBS-T for 10 min followed by TBS for 20 min. Nuclei were stained using 0.5 μg ml^{-1} DAPI (Sigma-Aldrich) for 5 min. Afterwards, sections were washed with TBS and mounted in *p*-phenylenediamine-glycerol to prevent photobleaching. The sections were coverslipped and sealed with nail polish. The slides were stored in a dark box at 4°C for up to 72 h with stable signal to noise ratio. Images were taken using a Zeiss Axioplan 2 imaging system equipped with Apotome stepper, Axiocam camera system and AxioVision 4.8 software.

Restraint stress protocol, tissue collection and plasma ACTH and corticosterone measurements

Restraint stress was used as a mixed physical and psychological stressor (Pacak & Palkovits, 2001). Mice were randomly assigned to one of two experimental groups assayed in parallel: control, non-stressed (basal) and restraint for 30 min (restraint). For restraint, mice were placed individually in a clear plastic restraint tube (CH Technologies (USA) Inc., Westwood, NJ, USA) of internal diameter 31 mm with a variable pusher, adjusted based on animal size. Mice were decapitated and trunk blood collected in chilled Eppendorf tubes containing 5 μl of 5% EDTA. Brains were rapidly isolated in ice-cold Hanks' buffered salt solution (HBSS, Invitrogen) and 1 mm coronal sections cut using a fresh razor blade. Hypothalamic blocks were then prepared by cutting along the top of the third ventricle and diagonally towards the ventral aspect to either side of the major hypothalamic nuclei, and then bisected in a sagittal plane. Anterior pituitary glands were sectioned on ice to produce two anterior lobes, removing the posterior and intermediate lobes, and individual adrenal glands were trimmed of fat. One half of each tissue or individual adrenal gland was stored at 4°C in RNAlater (Ambion Inc., Austin, TX, USA) overnight to ensure tissue penetration and then frozen at −80°C until use. Blood samples were chilled on ice and centrifuged at 1000 *g* for 10 min, and plasma was separated and stored at −80°C until subsequent radioimmunoassay for ACTH and corticosterone. Plasma ACTH and corticosterone concentrations were determined by radioimmunoassay using commercially available kits (MP Biomedicals, Solon, OH, USA). ACTH was measured in unextracted plasma samples using a two-site immunoradiometric assay (Hodgkinson *et al.* 1984). Corticosterone was measured in unextracted plasma (diluted 1:200 in assay buffer) using a double antibody radioimmunoassay with ^{125}I-labelled corticosterone as the tracer (Keith *et al.* 1978). Sensitivities were 5 pg ml^{-1} and 0.5 ng ml^{-1} and the intra-assay variation <8% and <6%, for the ACTH and corticosterone assays, respectively.

qRT-PCR

Tissue samples stored at −80°C in RNAlater were rapidly thawed at room temperature, weighed, and disrupted through a 21G needle using ∼20 strokes for hypothalamus and pituitary and ∼40 strokes for adrenal glands. RNA was then purified using RNeasy Mini Kit (Qiagen) or High Pure RNA Tissue Kit (Roche Applied Science) as per the manufacturer's instructions. RNA concentrations were determined using a Nanodrop (Thermo Scientific). cDNA was synthesised using Transcriptor High Fidelity cDNA Synthesis Kit (Roche Applied Science) using ∼2 μg of RNA. Reactions were primed with a 1:2 ratio mix of oligo-dT and random hexamers and incubated at 50°C for 30 min before inactivation at 85°C for 5 min. Control cDNA syntheses were performed in parallel including no reverse transcriptase enzyme control and no template RNA control.

qRT-PCR was performed on an Applied Biosystems Prism 7000 real-time PCR machine using SYBR Green JumpStart Taq Ready Mix (Sigma) in a 25 μl total volume reaction. Reactions were performed in triplicate with cycling as follows: 50°C for 2 min, 95°C for 10 min then 40 cycles of 95°C for 15 s and 60°C for 1 min under standard cycling conditions. PCR controls (no template, no enzyme, no primer, etc.) and template from cDNA synthesis controls were performed in parallel. mRNA expression was quantified relative to β-actin using the $\Delta\Delta C_t$ method (Livak & Schmittgen, 2001; Yuan *et al.* 2006; Bustin *et al.* 2009). Commercially available qRT-PCR primers were used (Qiagen) except for Kcnn1–4 that were designed and validated in-house with the following sequences:

Kcnn1 fwd CATCAgCCTgTCCACTgTCATCTTg; Kcnn1 rev gTCgTCggCACCATTgTCCAC; Kcnn2 fwd

ATCTTCggCATgTTCggCATCg; Kcnn2 rev ATCgTggAg AgACTgATAAggCATTTC; Kcnn3 fwd gCTTgTCCATCC TggTCTgTTgC; Kcnn3 rev ATggCggTAgAgTTgg CTgAAgTg; Kcnn4 fwd ggTTCTgCACgCTgAgATgTTg; Kcnn4 rev AAggCAgTggACAgggTgATC

Single cell RT-PCR

The cellular contents of single, fluorescently labelled corticotrophs that had been maintained in culture for 4 days were aspirated into RNAse free borosilicate patch-pipettes containing 7 μl of RNAse-free water. Aspirant was immediately transferred to an Eppendorf tube for cDNA synthesis using Sensiscript reverse transcriptase (Qiagen), RNasin ribonuclease inhibitor (Promega, Madison, WI, USA) and a mix of random and poly-dT primers in a final volume of 20 μl at 37°C for 1 h. For single cell PCR analysis, a two-stage PCR amplification strategy was used. Firstly, 2.5 μl of cDNA generated from the single cell aspirate was used in a 25 μl reaction using the SYBR Green JumpStart Taq Ready Mix and primers as for qRT-PCR. Samples were heated to 50°C for 2 min followed by 10 min at 95°C before performing 40 cycles at 95°C for 15 s and 60°C for 1 min standard cycling conditions on an ABI 7000. An aliquot (2.5 μl) of the first round amplification was then diluted into a new 25 μl PCR reaction and subjected to a further 10 amplification cycles using the conditions above. Multiple negative controls including control cell aspirants for which no reverse transcriptase was added (no-RT), aspiration of extracellular medium adjacent to intact cells (bath) and PCR controls were run in parallel with no detectable amplicon under identical conditions. Amplicons from the end-point PCR analysis were run on a 2% agarose gel and visualised using RedSafe (iNtRON Biotechnology, Kyungki-Do Korea). The predicted amplicon size (bp) for each primer set was: Kcnn1 = 94, Kcnn2 = 119, Kcnn3 = 75, Kcnn4 = 93, Kcnma1 = 106, Pomc = 99.

ACTH secretion *in vitro*

ACTH secretion *in vitro* was evaluated using dispersed anterior pituitary cells in static incubation assays. Dispersed anterior pituitary cells were prepared and transduced with lentivirus as above and plated in 96-well cluster dishes. Forty-eight to seventy-two hours post-transduction, cells were washed in Dulbecco's modified Eagle's medium (Invitrogen) containing 25 mM Hepes (Sigma-Aldrich) and 0.1% bovine serum albumin (BSA; Sigma-Aldrich) (DMEM-BSA), incubated for 2 h at 37°C in a water bath. Cells were then exposed to vehicle (basal) or 0.1 nM CRH + 2 nM AVP in the presence or absence of the respective ion channel inhibitor for 30 min. Plates were then placed on ice and the supernatant removed, spun briefly at 100 *g*, snap frozen on dry ice and stored at −70°C until radioimmunoassay. ACTH was determined, in duplicate, using a commercial radioimmunoassay kit (ACTH kit RK-001–21, Phoenix Pharmaceuticals Inc., Belmont, CA, USA) following appropriate dilution in radioimmunoassay buffer.

Corticotroph action potential model

The model is adapted from the original corticotroph action potential model from LeBeau *et al.* (1997), incorporating some of the adaptations made by Shorten *et al.* (2000). The original model simulates membrane potential using a set of Hodgkin–Huxley-type equations representing L-type and T-type voltage sensitive Ca^{2+} currents, a delayed rectifier (K-DR), a Ca^{2+} activated K^+ current (K-Ca), and a leak current representing the remaining ionic currents. It does not include a voltage-activated sodium conductance. It includes a basic representation of intracellular Ca^{2+}, sufficient to model the calcium-activated channels, assuming uniform spatial distribution of Ca^{2+}. We have developed the Le Beau model by adding a voltage sensitive A-type K^+ current (K-A) and replacing the leak current with a background, non-selective predominantly conducting Na^+ current (NS-Na) and an inward rectifying K^+ current (K-IR). The modelled K-A current is based on Tabak *et al.* (2007) and the NS-Na current is based on the formulation of Tsaneva-Atanasova *et al.* (2007). Our K-IR current uses a different formulation from Shorten *et al.* (2000), based instead on the somatotroph model of Tsaneva-Atanasova *et al.* (2007). In each case we have used their parameter values as a base and then adjusting to match our own recordings, looking at the detailed form of the action potentials. We have also added some Gaussian noise to the model's membrane potential, in order to more closely compare with the irregular recorded data. The noise is generated using an Ornstein–Uhlenbeck process (essentially integration step size scaled Gaussian noise with exponential decay), controlled by amplitude and decay parameters, o_A and o_d.

Parameters controlling calcium- and voltage-dependent time courses were shifted in order to match the time scale of our observed action potentials. The action potentials in the LeBeau model are very much slower, on a scale of ∼100 ms compared to our *in vitro* action potentials of ∼20 ms. To shorten these we increased the Ca^{2+} buffering factor from 0.01 to 0.2, reduced the Ca^{2+} exchange time constant from 500 ms to 110 ms, and shifted the voltage dependence of Ca^{2+} channel (L-type and T-type) gating in the negative direction (LeBeau *et al.* 1997).

Model equations for K-IR, NS-Na and K-A. The K-IR current is described by:

$$I_{\mathrm{K-IR}} = g_{\mathrm{K_{IR}}} K_{\mathrm{IR}_\infty} \Phi_K$$

where Φ_K is the K^+ driving force described in LeBeau *et al.* (1997) and the steady state activation $K_{IR,\infty}$ is described:

$$K_{IR\infty} = \frac{\alpha_{IR}}{\alpha_{IR} + \beta_{IR}}$$

$$\alpha_{IR} = \frac{0.1}{1 + exp(0.06(V_m - V_{IR} - 200)}$$

$$\beta_{IR} = \frac{3\exp[0.0002(V_m - V_{K_{IR}} + 100)] + \exp[0.1(V_m - V_{K_{IR}} - 10)]}{1 + \exp[-0.5(V_m - V_{K_{IR}})]}$$

The non-selective predominantly Na^+-conducting current (NS-Na) uses a very simple form:

$$I_{NSNa} = g_{NSNa}(V_m - V_{NSNa})$$

The fast-inactivating, voltage sensitive A-type K^+ current is described by:

$$I_A = g_A m_{A_\infty} h_A \Phi_K$$

with steady state activation $m_{A,\infty}$ and inactivation $h_{A,\infty}$ is described:

$$m_{A_\infty} = \frac{1}{1 + \exp[(V_{m_A} - V_m)/k_{m_A}]}$$

$$\frac{dh_A}{dt} = \frac{h_{A\infty}(V) - h_A}{\tau_{h_A}}$$

$$h_{A_\infty}(V) = \frac{1}{1 + \exp[(V_{h_A} - V)/k_{h_A}]}$$

Adding these currents to the LeBeau *et al.* (1997) model and removing the leak current gives the new membrane potential (V) equation:

$$\frac{dV}{dt} = \frac{(I_{Ca-L} + I_{Ca-T} + I_{K-DR} + I_{K-Ca} + I_{K-IR} + I_A + I_{NSNa}) + \text{noise}}{c_m}$$

The equations were integrated with the Runge–Kutta method, using a 0.1 ms step size.

Statistics

All data are expressed as means ± SEM with n = number of individual experiments or cells. Data were analysed using a parametric one-way ANOVA with *post hoc* Dunnett's test or non-parametric Kruskal–Wallis test as appropriate using Igor Pro v6.0 (Wavemetrics) or GraphPad Prism 5 (GraphPad Software Inc., La Jolla, CA, USA) with significant differences between groups defined at $^*P < 0.05$ or $^{**}P < 0.01$.

Reagents

Salts and biochemical reagents for electrophysiological analysis, including channel inhibitors, were from Sigma-Aldrich Co. (Poole, UK) and of the highest analytical grade unless specified otherwise in the methods. CRH and AVP were from Bachem Ltd (Weil am Rhein, Germany). Cell culture media including DMEM, HBSS, PBS and fetal calf serum were from Gibco Invitrogen Ltd (Paisley, UK)

Results

Labelling of corticotrophs *in vitro* using a lentiviral-driven POMC-eYFP reporter

To allow specific labelling of corticotrophs *in vitro* for patch clamp electrophysiological analysis we expressed eYFP under the control of a minimal POMC promoter using lentivirus-mediated cell transduction of isolated anterior pituitary cells *in vitro* (Fig. 1*A*). Using the minimal POMC promoter greater than 95% of corticotrophs that were immunohistochemically identified as ACTH-expressing cells from the murine anterior pituitary gland expressed the eYFP reporter. In contrast, using the constitutive CMV promoter less than 30% of the ACTH positive cells expressed eYFP (Fig. 1*B*) demonstrating the efficiency of lentiviral-mediated expression of eYFP in corticotrophs. The specificity of the minimal POMC-promoter driven expression of eYFP for ACTH positive cells was greater than 99.5% (Fig. 1*C*), presenting an ideal approach for the unequivocal identification of living murine anterior pituitary corticotrophs. Importantly, lentiviral mediated-transduction of corticotrophs with eYFP did not compromise basal or secretagogue-induced ACTH secretion, as measured by RIA (Fig. 1*D*), indicating that corticotroph viability and function were not compromised by our identification approach.

Murine corticotrophs are spontaneously active with heterogeneous firing patterns

The specific labelling of corticotrophs with eYFP allowed us to examine the spontaneous electrical activity of naive cells. Preliminary experiments using conventional whole cell recording resulted in a rapid (within a few minutes) cessation of spontaneous firing, and thus all subsequent analyses were performed using the perforated patch-clamp version of the whole-cell recording technique. Under these conditions of metabolically intact cells more than 95% of all cells displayed spontaneous electrical excitability that was maintained for the duration (typically >30 min) of the recording. The mean cell capacitance was 4.56 ± 0.32 pF,

mean resting membrane potential -55.0 ± 1.7 mV, and typical input resistance >3 GΩ ($n > 100$ cells).

The high input resistance of these cells would imply that small fluctuations in membrane current would have a significant impact on membrane potential. Accordingly, there was very considerable variability in action potential firing patterns between cells even from the same batch of cells recorded on the same day (Fig. 2). Furthermore, similar heterogeneity was also observed in corticotrophs isolated from POMC-GFP mice in current clamp using the perforated patch mode of recording (not shown). Previous studies analysing spontaneous action potentials in corticotrophs are conflicting. For example, rat corticotrophs are reported to be either spontaneously active (Kuryshev *et al.* 1997) or electrically silent (Lee & Tse, 1997). This might reflect either the recording conditions (perforated patch *vs.* whole-cell respectively) or cell isolation procedure used. Indeed, we found that in pilot studies conventional whole-cell approaches led to rapid run-down of spontaneous activity. This is in agreement with a recent study (Lee *et al.* 2011) using whole-cell recording from corticotrophs isolated from transgenic mice overexpressing GFP under control of the POMC promoter, in which corticotrophs appear to be predominantly electrically silent.

The majority of cells in our perforated-patch clamp studies displayed large amplitude single action potential spikes of variable frequency (Fig. 2*A* and *B*). Analysis of single spikes from different corticotrophs revealed a bimodal distribution in the amplitude of the after-hyperpolarisation following the spike (Fig. 3*A* and *B*). We thus categorised single spikes as either type A (Fig. 2*A*), in which the AHP was >25 mV, or type B (Fig. 2*B*) with AHP amplitude <20 mV. The proportion of cells displaying type A spikes was similar to that displaying type B spikes (~40%). Cells displaying type A or B spikes typically had similar resting membrane potentials in the range of -50 mV with no significant differences in spike threshold or spike amplitude (Fig. 3*A*, *C*, *D* and *F*). In addition, the mean cell capacitance (type A: 4.58 ± 0.31 pF, type B: 4.55 ± 0.38 pF) or input resistance (type A: 5.28 ± 0.51 GΩ, type B 5.25 ± 0.43 GΩ) of cells that displayed type A or type B spikes was not significantly different. However, type B spikes displayed a slower time

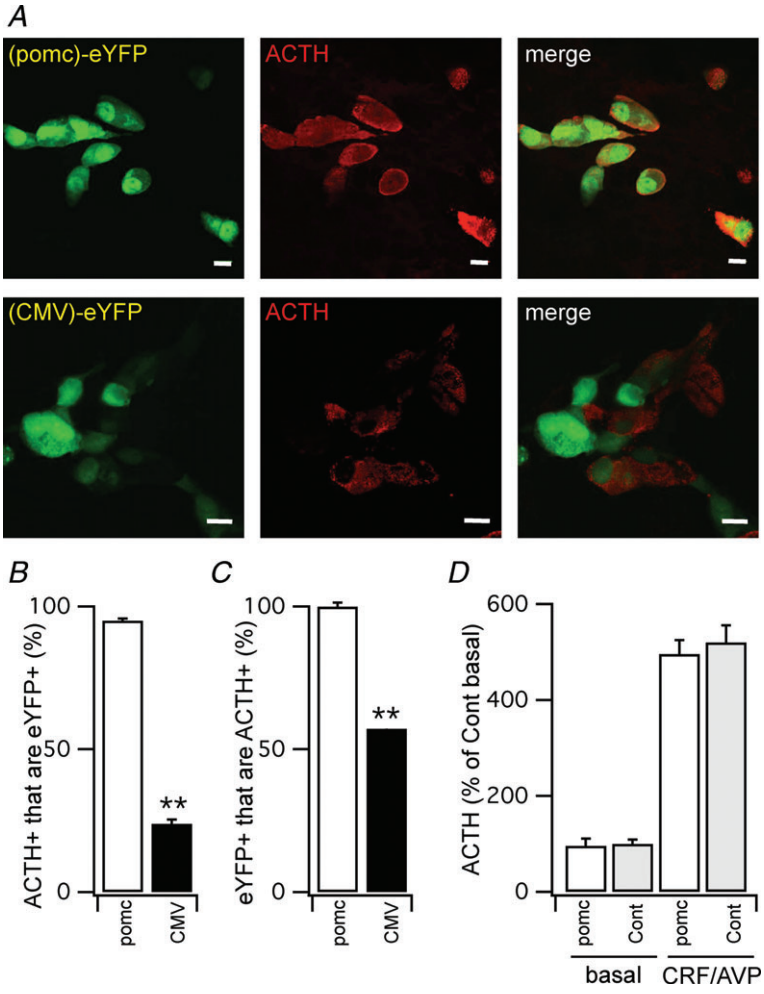

Figure 1. Labelling of murine corticotrophs *in vitro* using lentiviral transduction of a POMC-eYFP fluorescent reporter
A, representative confocal sections of dispersed anterior pituitary cells in primary culture 4 days following transduction with pomc-eYFP (top panels) or CMV-eYFP (bottom panels). The eYFP signal (left panels), ACTH immunoreactivity (middle panels) and merged images are shown. Scale bar is 10 μm. *B*, quantification of percentage of cells immunoreactive for ACTH (ACTH+) that are also labelled with eYFP (eYFP+) using either the POMC- or CMV- promoter lentiviral constructs. *C*, quantification of percentage of cells labelled with eYFP (eYFP+) that are also immunoreactive for ACTH (ACTH+) and that are also using either the POMC- or CMV-promoter lentiviral constructs. *D*, ACTH release from control (Cont) and POMC-eYFP (POMC) transduced cultures under basal and stimulated (CRH/AVP, 0.1 and 2 nM respectively) expressed as a percentage of the basal release in control (non-transduced) cultures. All data are means ± SEM, $n > 3$ independent experiments.

to peak (Fig. 3*E*), increased spike width (Fig. 3*G*) as well as a smaller afterhyperpolarisation amplitude (Fig. 3*H*) compared to type A spikes.

While cells rarely spontaneously converted between type A and type B action potentials, spike frequency during recordings varied considerably, ranging from <0.1 Hz to several hertz. Furthermore, cells with type A or B spikes also displayed spontaneous, reversible transitions to 'pseudo-plateau bursting modes', in which action potentials, of variable amplitude may be superimposed on periodic depolarized potentials (e.g. Fig. 2*C*–*H*) as described in other anterior pituitary cells (Tabak *et al.* 2007; Tsaneva-Atanasova *et al.* 2007). In a low proportion (<5%) of cells 'pseudo-plateau bursts' were observed during recordings (∼30 min) devoid of single spike events.

Exposure of corticotrophs to a brief pulse (3 min) of the combined secretagogues CRH and AVP (at 0.1 nM and 2 nM respectively, concentrations approximating those released into the portal circulation in response to stress; Gibbs & Vale, 1982; Sheward & Fink, 1991) resulted in a rapid increase in the frequency of action potential firing, with a concomitant steady depolarisation from rest of 14.6 ± 5.5 mV ($n = 5$), measured at 2 min after CRH/AVP application (Fig. 4*A*–*C*). The membrane

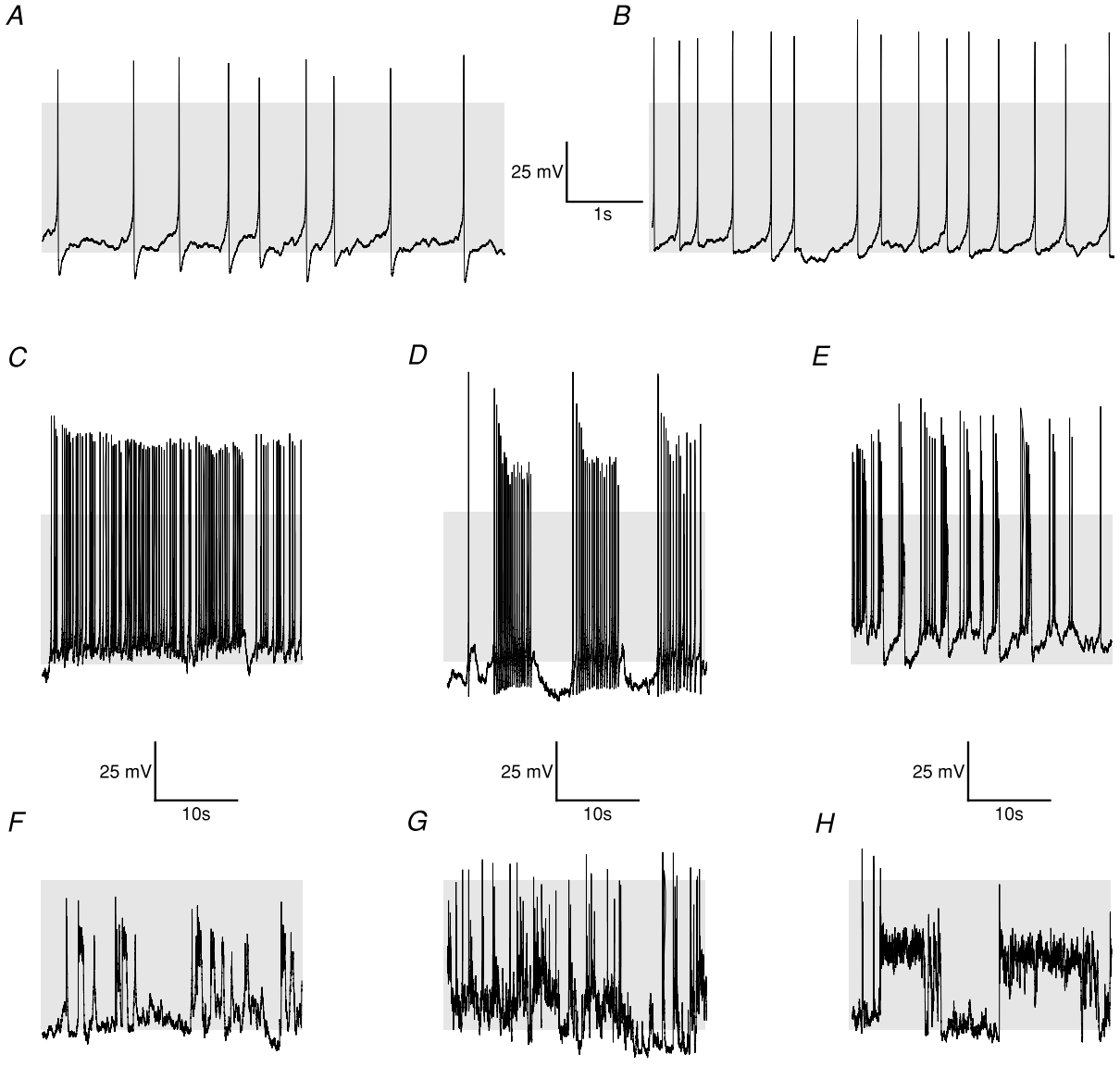

Figure 2. Heterogeneity of spontaneous electrical activity in murine corticotrophs
Waveforms and firing patterns differed widely between cells, and individual cells could transition between firing patterns. In perforated-patch clamp recordings the majority of cells exhibited spontaneous tall spikes, falling into one of two categories, as depicted in *A* (Type A; >30% of cells) and *B* (type B; >40% of cells). Detailed differences between these waveform types are elaborated upon in Fig. 3. Cells spontaneously and reversibly transitioned to other firing patterns represented by panels *C*–*H*, including 'pseudo-plateau potential' bursting behaviours. Grey shading indicates membrane potential between −50 and +10 mV.

depolarisation and increase in action potential frequency were maintained upon washout of the secretagogues. The mean time to full recovery to the preceding (unstimulated) membrane potential was 20.3 ± 4.2 min ($n = 4$).

A background sodium conductance controls resting membrane potential

In a proportion of cells we could detect TTX-sensitive fast inactivating inward currents; however current amplitude was highly variable. TTX modified the amplitude of the tallest spike events but had no significant effect on spikes that did not reach above 0 mV (data not shown). On the whole, TTX (1–2 μM) did not typically alter the probability or frequency of spike generation in these cells, in agreement with previous studies in rat corticotrophs (Kuryshev *et al.* 1997).

In several pituitary types, spontaneous activity is dependent on a non-voltage gated (and TTX-insensitive) inward sodium conductance (Simasko, 1994; Takano *et al.* 1996; Tomic *et al.* 2011). In our studies, replacement of external Na^+ ions with the large impermeant organic cation *N*-methyl-D-glucamine ($NMDG^+$) was accompanied by a rapid and reversible hyperpolarisation of the membrane potential resulting in cessation of spontaneous action potential firing (Fig. 5*A*). In voltage clamp recordings, in which cells were held at the potassium reversal potential, replacement of external Na^+ with $NMDG^+$ resulted in inhibition of a standing inward current (Fig. 5*B*). This suggests that a background inward sodium conductance maintains the resting membrane potential of murine corticotrophs in a relatively (∼−55 mV) depolarised state. As removal of extracellular Na^+ prevents any inward sodium conductance, we cannot, however, exclude that other voltage-dependent, TTX-insensitive sodium conductances also contribute to the rising phase of spontaneous action potentials.

Replacement of external Na^+ with $NMDG^+$ also prevented the rapid CRH/AVP-induced depolarisation of the cell and increases in CRH/AVP-stimulated action potential firing. At 2 min following addition of CRH/AVP, in the continued presence of NMDG, the mean

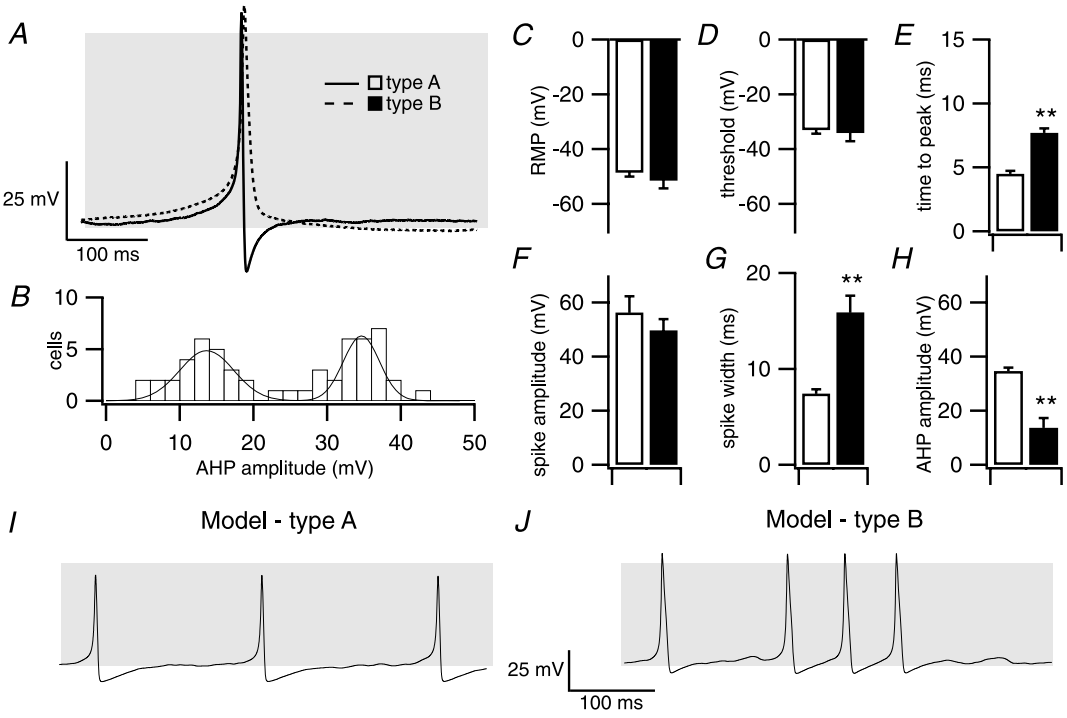

Figure 3. Characterisation of type A and type B action potentials.
Several features of type A and type B action potential waveforms differed concurrently between cells. *A*, averaged traces from type A (continuous line, open square) and type B (dashed line, filled square) action potentials as in Fig. 2. *B*, histogram of afterhyperpolarisation (AHP) amplitude from single spikes demonstrates a bimodal distribution. Spikes with an AHP amplitude >25 mV were defined as type A spikes. *C–H*, mean resting membrane potential (*C*), threshold for action potential generation (*D*), time to action potential peak (*E*), spike amplitude (*F*), spike width (*G*) and afterhyperpolarisation amplitude (*H*) for type A and B spikes. *I* and *J*, modelling of type A (*I*) and type B (*J*) action potentials using a revised formulation of a corticotroph action potential model that incorporates additional conductances identified in this study. Grey shading indicates membrane potential between −50 and +10 mV. Data are means ± SEM, $n = 19$ per group. $^{**}P < 0.01$, ANOVA with *post hoc* Dunnett's test compared to type A spikes.

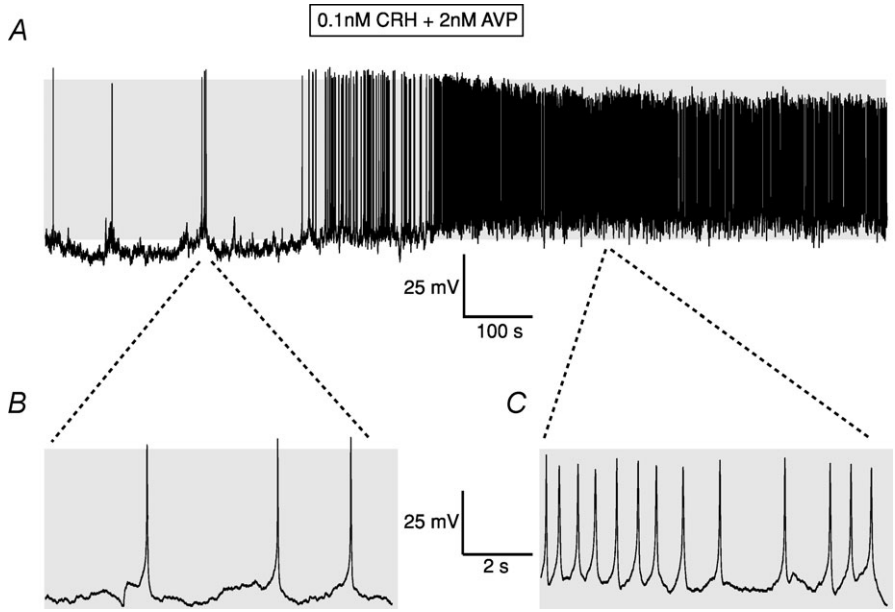

Figure 4. Stimulation of murine corticotrophs by CRH/AVP
A, representative current clamp recording of a metabolically intact corticotroph before and following exposure to a 3 min pulse of 0.1 nM CRH and 2 nM AVP. *B* and *C*, expanded traces before application of CRH/AVP (*B*) and immediately following washout of secretagogue (*C*). Grey shading indicates membrane potential between −50 and +10 mV.

depolarisation was only 2 ± 3 mV, $n = 5$, significantly smaller than that observed in physiological extracellular Na^+ solutions (Fig. 5*C*). In the continued presence of NMDG and CRH/AVP there was, however, a significantly delayed depolarisation, peaking to 18.1 ± 2.7 mV after 12.9 ± 1.7 min. The identity of this CRH/AVP-regulated conductance is unknown. However, the time course suggests it may contribute to the sustained depolarisation

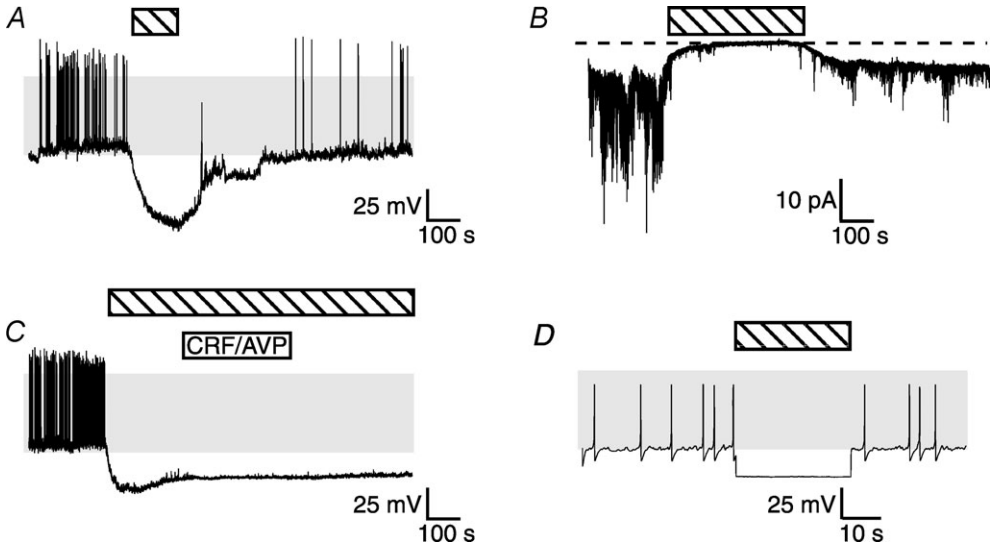

Figure 5. A background sodium conductance contributes to resting membrane potential
Effects of substitution of external Na^+ with the impermeant ion $NMDG^+$, indicated by the horizontal hatched bar, during perforated patch recordings. TTX at 2 μM is present throughout. *A*, $NMDG^+$ substitution for Na^+ causes hyperpolarization and cessation of action potential generation. *B*, voltage clamp at the K^+ reversal potential reveals a standing inward conductance that is eliminated during $NMDG^+$ substitution. *C*, CRH/AVP does not rapidly depolarise corticotrophs or stimulate action potential generation in Na^+-free external solutions. *D*, in the mathematical model of a corticotroph, elimination of the background Na^+ conductance simulates the recording shown in *A*.

and increase of action potential firing upon washout of CRH/AVP under physiological conditions.

Modelling spontaneous activity of murine corticotrophs

In previous models of corticotroph excitability (LeBeau *et al.* 1997; Shorten *et al.* 2000), some key aspects of action potential properties and bursting were studied that do not accurately predict the observed resting membrane potential of murine corticotrophs or the variability in duration of action potential waveform. For example, mean resting potential is at or below −70 mV in these models, potentials rarely reached in murine corticotrophs. This is likely to reflect that current models do not include the NMDG-sensitive background sodium conductance that maintains the resting membrane potential of murine corticotrophs around −55 mV. We thus modified the LeBeau model to incorporate a sodium-dependent non-selective inward conductance (NS-Na) with additional conductances (including an inactivating A-type conductance (K-A) and inwardly rectifying conductance (K-IR), based on our analysis of potassium conductances in murine corticotrophs as below). In our revised model, the K-IR and NS-Na currents act against each other to control the cell's resting membrane potential and excitability. To simulate our recordings their conductances were balanced against each other and we introduced Gaussian noise to simulate the variability in firing patterns. In the model, too much K-IR prevents firing, and too much NS-Na prevents the cell from repolarising, maintaining a high plateau potential. We could thus simulate typical resting membrane potentials in murine corticotrophs (range −60 to −50 mV), with concomitant action potential firing, by increasing NS-Na and then increasing K-IR in parallel to preserve firing activity. Under these conditions, the shift from type A to type B action potentials could be accurately modelled by reducing both the A-type and calcium-sensitive potassium channel conductances (Fig. 3*I* and *J*). Furthermore, in agreement with our electrophysiological recordings from spontaneously active cells, inhibition of the inward sodium conductance (NS-Na) resulted in cell membrane hyperpolarisation and cessation of action potential firing (Fig. 5*D*).

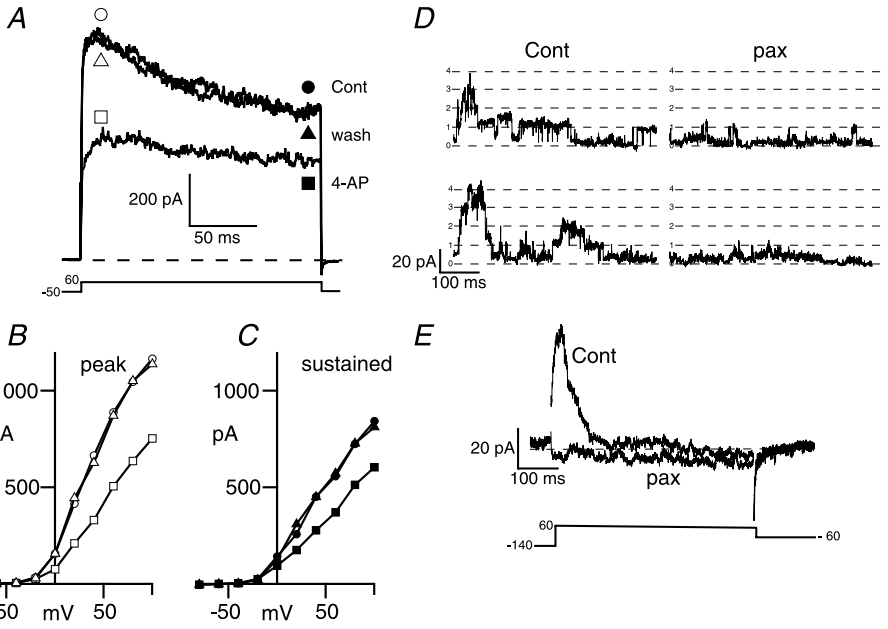

Figure 6. A-type voltage-gated potassium channels and large conductance calcium-activated potassium (BK) channels are expressed in corticotrophs.
A, representative voltage-clamp recording of a metabolically intact corticotroph displaying significant inactivating outward current when depolarised from a holding potential of −50 mV to +60 mV before (cont, circles) during (4-AP, squares) and after washout (wash, triangles) with 4-aminopyridine (4-AP, 1 mM) an inhibitor of A-type potassium channels. *B* and *C*, current–voltage relationship for the cell in *A* determined at the peak outward current shown by the open symbols in *A* (*B*) or during the sustained phase (180–200 ms into pulse) shown by the filled symbols in *A* (*C*). *D*, single channel recordings from inside-out membrane patches exposed to 5 μM intracellular free calcium determined during a step pulse to +60 mV before (Cont) and after application of the specific BK channel inhibitor paxilline (pax, 1 μM). *E*, ensemble average traces in the presence and absence of paxilline from 15 recordings as in *D*.

Murine corticotrophs express multiple potassium channels

Murine corticotrophs display large outward currents at positive potentials under the perforated patch conditions used with inactivating and non-inactivating components dominating in different cells (compare, for example, Fig. 6*A* and Fig. 7*A*). To investigate the contribution of different potassium conductances we took a pharmacological approach and analysed the effects of various potassium channel inhibitors on the outward current.

Previous studies in murine AtT20 D16:16, as well as rat, corticotrophs have reported an A-type inactivating potassium conductance sensitive to 4-aminopyridine (4-AP) (Pennington *et al.* 1994; Lee & Tse, 1997). At 1 mM, 4-AP is relatively selective for A-type potassium channels. At this concentration it inhibited the peak outward current (Fig. 6*B*) during the pulse by 36.7 ± 2.8% ($n = 16$, determined at +40 mV) whereas the sustained current (Fig. 6*C*) was only reduced by 15.1 ± 6.0% ($n = 16$). Raising 4-AP to 10 mM resulted in an inhibition of sustained and peak outward potassium current by 73.1 ± 2.8% ($n = 5$) and 75.3 ± 3.1% ($n = 5$), respectively.

Application of 1 mM TEA inhibited the outward sustained current by 31.9 ± 4.6% ($n = 6$). This concentration is relatively selective for large conductance calcium activated potassium channels in some systems. However, application of 1 μM paxilline, the specific BK channel inhibitor, blocked only a small and variable proportion of the outward sustained current (mean 11.5 ± 2.3%, range 5–28%, $n = 14$) and 18.3 ± 3.2% ($n = 14$) of the peak current, suggesting a relatively modest contribution of BK channels to the outward current under the recording conditions used. In inside-out patch recordings, in the presence of 5 μM intracellular free calcium, a step depolarisation to +60 mV, from a holding potential of −140 mV, revealed activation of large conductance (~300 pS) BK channels, at the start

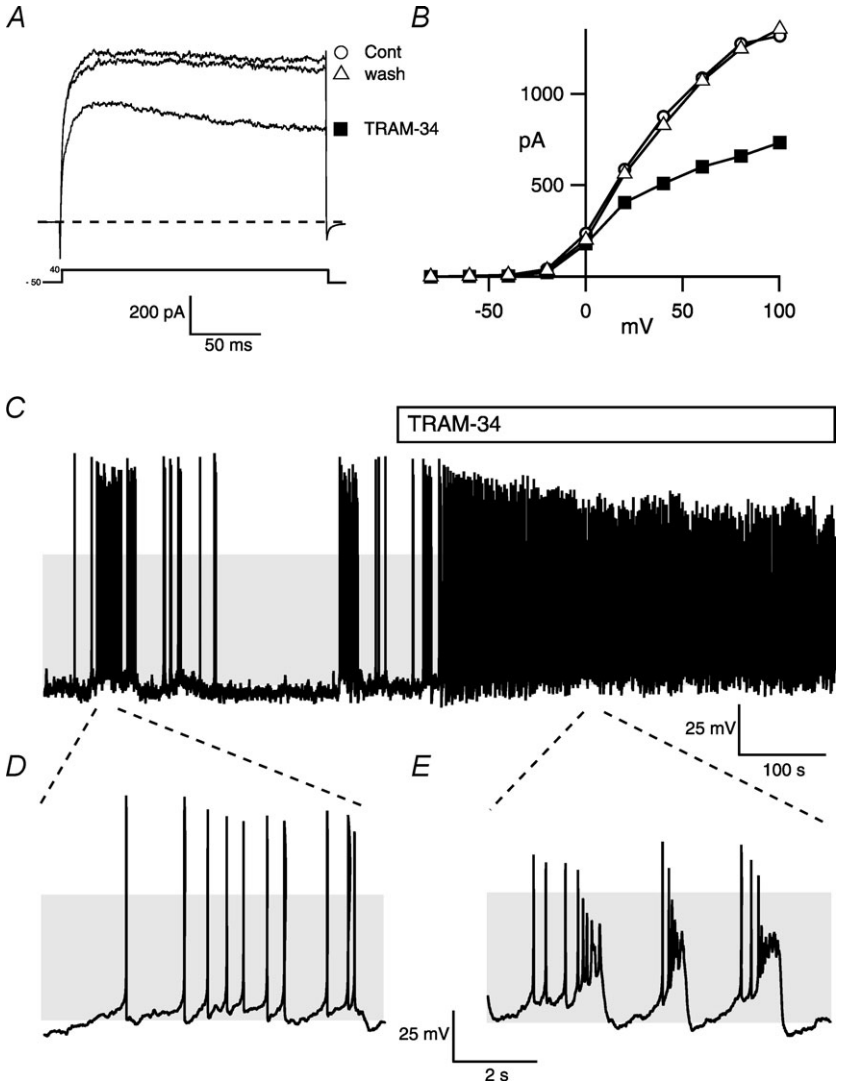

Figure 7. TRAM-34 sensitive intermediate conductance calcium-activated potassium channels (SK4) control corticotroph excitability
A, representative voltage-clamp recording of a metabolically intact corticotroph depolarised from a holding potential of −50 mV to + 40 mV before (cont, open circle) during (TRAM-34, filled square) and after washout (wash, open triangle) of the specific inhibitor of intermediate conductance calcium activated potassium (SK4) channels, TRAM-34 (1 μM). *B*, current–voltage relationship of the whole cell outward current from the cell in *A*. *C–E*, representative current-clamp recording of a metabolically intact corticotroph before and during exposure to TRAM-34 (*C*), with expanded traces before (*D*), and during exposure to TRAM-34 (*E*). Grey shading indicates membrane potential between −50 and +10 mV.

of the pulse that inactivated (t_{half} of 51.5 ± 6.0 ms over the time course of the pulse (Fig. 6*D*). Paxilline (1 μM) blocked 89.4% of this current, as determined from ensemble averages from 15 individual sweeps (Fig. 6*D* and *E*). Furthermore, BK channel activity was essentially abolished under these conditions upon perfusion of a nominally (EGTA buffered) calcium free intracellular solution to the intracellular face of the patch (not shown). Thus, while BK channels are expressed in murine corticotrophs their contribution to the outward current is modest under normal resting membrane conditions in metabolically intact corticotrophs.

To test whether other calcium-activated potassium conductances are expressed in murine corticotrophs we first examined the effect of 500 nM apamin. Apamin blocks a variety of small conductance calcium-activated potassium (SK) channels that are reported to be activated by AVP in rat corticotrophs (Tse & Lee, 1998). In 8/9 cells application of apamin elicited a small but significant (mean inhibition was 11.3 ± 8.4%, $n = 9$, $P < 0.05$ Student's paired *t* test) inhibition of the sustained outward current. In contrast, 1 μM clotrimazole, at a concentration that blocks intermediate conductance calcium-activated (SK4) potassium channels, inhibited the sustained outward current by 39.8 ± 3.5% ($n = 9$). However, at concentrations above 1 μM clotrimazole has been reported to be non-selective for SK4 channels (Wulff *et al.* 2000); thus we examined the effect of the selective SK4 inhibitor 1-[(2-chlorophenyl)diphenylmethyl]-1*H*-pyrazole (TRAM-34; Fig. 7*A* and *B*). TRAM-34 inhibited the sustained outward current, determined at +40 mV, by 37.6 ± 3.8% ($n = 5$), a value similar to that observed with clotrimazole.

Taken together these data demonstrate that murine corticotrophs express multiple outward potassium conductances and that in perforated patch recordings the calcium-activated intermediate conductance potassium channel, sensitive to TRAM-34, mediates a significant proportion of the outward current.

Murine corticotrophs also express an inwardly rectifying potassium conductance (Fig. 8*A*) that is blocked more than 50% by 100 μM external Ba^{2+}, as previously reported in rat corticotrophs (Kuryshev *et al.* 1997). In corticotrophs from male rats, the Ba^{2+}-sensitive inwardly rectifying potassium conductance has been implicated in controlling both spontaneous and CRH-induced corticotroph depolarisation and enhanced action potential frequency. However, 100 μM Ba^{2+} had no significant effect on murine corticotroph depolarisation or action potential frequency in any cell (6/6) examined (Fig. 8*B*).

Intermediate conductance calcium-activated potassium channels regulate corticotroph excitability and ACTH secretion *in vitro*

Since a large component of the outward potassium current was carried via the TRAM-34 sensitive current in murine corticotrophs, we further analysed whether SK4 channels control corticotroph excitability and/or ACTH secretion. In 4/6 corticotrophs, exposure to TRAM-34 resulted in a significant increase (4.7 ± 1.8-fold, $n = 4$ determined from the 2 min immediately preceding and following TRAM-34 exposure) in action potential frequency that was typically associated with a transition to a pseudo-plateau bursting phenotype (Fig. 7*C*–*E*). In the presence of TRAM-34 the duration of the plateau burst, the number of spikes per burst and interspike interval across the spontaneous bursts were highly variable even in the same cell as well as between responding cells. Furthermore, in contrast to the effect of CRH/AVP, the change in action potential frequency and 'pseudo-plateau bursting' seen with TRAM-34 was not associated with a significant and sustained depolarisation of the resting membrane potential. In the four cells that responded with an

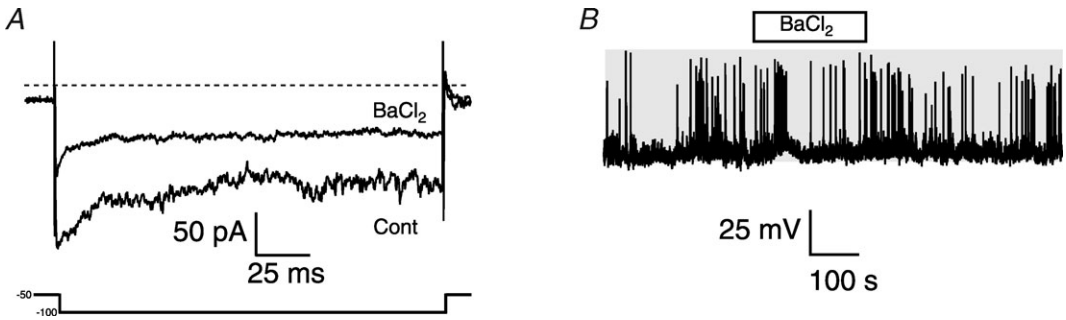

Figure 8. Barium-sensitive inwardly rectifying potassium conductance does not control action potential generation in murine corticotrophs
A, representative voltage-clamp recording of a metabolically intact corticotroph in the presence of elevated (20 mM) extracellular potassium and step hyperpolarised from −50 mV to −100 mV before (Cont) and after addition of 100 μM $BaCl_2$ to the bath. *B*, current-clamp recording of corticotroph in physiological extracellular solution exposed to 100 μM $BaCl_2$ (horizontal open bar). Note lack of Ba^{2+} on firing. Grey shading indicates membrane potential between −50 and +10 mV.

increase in activity following exposure to TRAM-34 the mean resting membrane potential increased by only 1.7 ± 2.1 mV compared to the pretreatment control period.

To examine whether SK4 channels affect ACTH secretion *in vitro*, we assayed basal and CRH/AVP stimulated ACTH release in static cultures in the presence and absence of clotrimazole or TRAM-34. Both clotrimazole and TRAM-34 alone induced a small, but significant ($P < 0.05$, Kruskal–Wallis with *post hoc* Dunnett's test) increase in basal ACTH output and induced a small potentiation of CRH/AVP stimulated ACTH release *in vitro*. A 30 min exposure to 0.1 nM CRH and 2 nM AVP stimulated basal ACTH release in static cultures 4.1 ± 0.3-fold ($n = 6$). TRAM-34 (1 μM) alone had a small but significant effect (Kruskal-Wallis with *post hoc* Dunnett's test, $P < 0.05$) increasing ACTH release to 1.4 ± 0.2 fold above basal levels. In the presence of TRAM-34 the effect of CRH and AVP was significantly potentiated compared to the effect CRH and AVP alone (to 5.2 ± 0.4-fold above basal levels in the absence of TRAM-34). As TRAM-34 potentiated rather than reduced the CRH/AVP-induced release of ACTH, this suggests that CRH/AVP does not regulate corticotroph excitability by inhibiting the TRAM-34 sensitive SK4 channels *per se*. Taken together these data support a role for SK4 channels as negative regulators of corticotroph excitability and ACTH secretion and point to a role for these channels in determining corticotroph and stress axis function.

Stress hyperresponsiveness in mice deficient for Kcnn4

To address whether SK4 channels play an important role in corticotroph function *in vivo* we examined the stress response in female mice lacking the SK4 channel (Kcnn4) (Sausbier *et al.* 2006). If SK4 channels play a significant role in ACTH release from the corticotroph *in vivo* we would predict that mice deficient for SK4 would display an exaggerated ACTH and corticosterone (CORT) release in response to an acute stress, i.e. a stress hyperresponsive phenotype in accordance with the exaggerated release of ACTH from corticotrophs *in vitro*. In mice with a global deletion of the pore exon of the Kcnn4 gene encoding SK4 channels (Kcnn4$^{-/-}$ mice) basal release of ACTH was not significantly different from wild-type (WT) age and litter matched female mice (Fig. 9*A*). Thirty minutes of restraint resulted in robust stimulation of plasma ACTH levels in WT by more than 3-fold. However, stress-induced plasma ACTH levels were significantly enhanced in Kcnn4$^{-/-}$ mice compared to WT controls, resulting in a more than 4-fold increase in plasma ACTH levels following restraint (Fig. 9*A*). These stress-induced changes in plasma ACTH were paralleled by changes in plasma CORT (Fig. 9*B*). Again, no significant difference in basal CORT levels was observed between genotypes. However, restraint stress-induced plasma CORT levels were significantly higher in Kcnn4$^{-/-}$ mice than in WT. Thus, both the ACTH and CORT response to restraint stress, but not basal output, are significantly enhanced in mice deficient for the Kcnn4 gene encoding the SK4 channel. This suggests that SK4 channels are more important for damping stress responses than for inhibiting basal HPA-axis function.

These data are in agreement with the *in vitro* effects of SK4 inhibition on evoked ACTH release, suggesting that the stress hyperesponsiveness observed in the Kcnn4$^{-/-}$ mice results, in part at least, from the loss of SK4 channels from corticotrophs. However, to examine whether Kcnn4 deletion may additionally exert effects at other levels of the HPA axis, or through additional mechanisms at the level of the anterior pituitary corticotroph, we used qRT-PCR to test for changes in gene expression in key HPA components in WT and Kcnn4$^{-/-}$ mice under basal and restraint stress conditions.

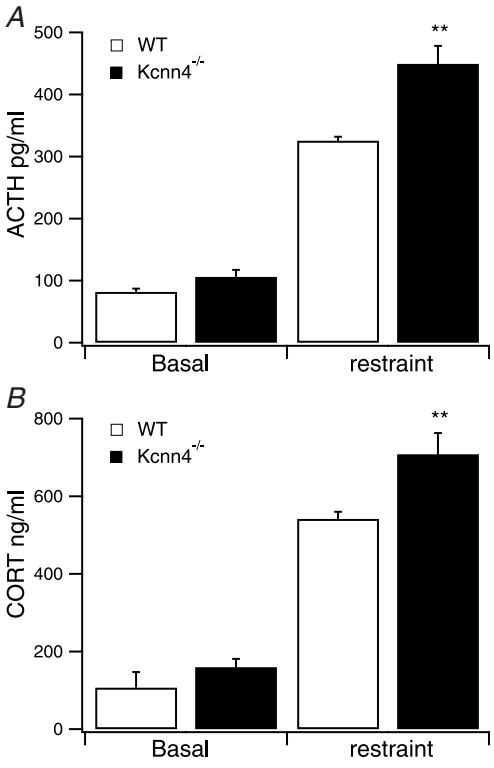

Figure 9. Enhanced restraint stress-induced plasma ACTH and corticosterone concentration in Kcnn4$^{-/-}$ knockout mice
A and *B*, plasma ACTH (*A*) and corticosterone (CORT) (*B*) concentrations under resting conditions (basal) and following 30 min of restraint stress (restraint) in wild-type (WT, open bar) and mice genetically deficient for the gene (Kcnn4) encoding SK4 channels (Kcnn4$^{-/-}$, filed bar). Data are means ± SEM, $n = 7$/group. $^{**}P < 0.01$, ANOVA with *post hoc* Dunnett's test compared to WT.

First, we examined tissue mRNA expression of Kcnn4 to confirm that Kcnn4 is expressed in the anterior pituitary and determine whether Kcnn4 is also expressed in the hypothalamus and adrenal gland. Kcnn4 mRNA was expressed in the hypothalamus, anterior pituitary and adrenal gland (Fig. 10*A*). However, mRNA levels were at least an order of magnitude below the mRNA expression for the related genes (Kcnn1–3) encoding small conductance calcium activated potassium channels (SK1–3). As expected, a qRT-PCR approach that was based on sequences, which have not been deleted in construction of the Kcnn4$^{-/-}$ mice resulted in a significant reduction (by approximately an order of magnitude) of Kcnn4 mRNA detected in all analysed tissues from the Kcnn4$^{-/-}$ mice. Importantly, knockout of Kcnn4 did not significantly affect mRNA expression of the related small conductance calcium activated channels SK1–3 in the hypothalamus, pituitary or adrenal (Fig. 10*A*). To verify that mRNA encoding for SK4 channels was expressed in corticotrophs we undertook single cell PCR.

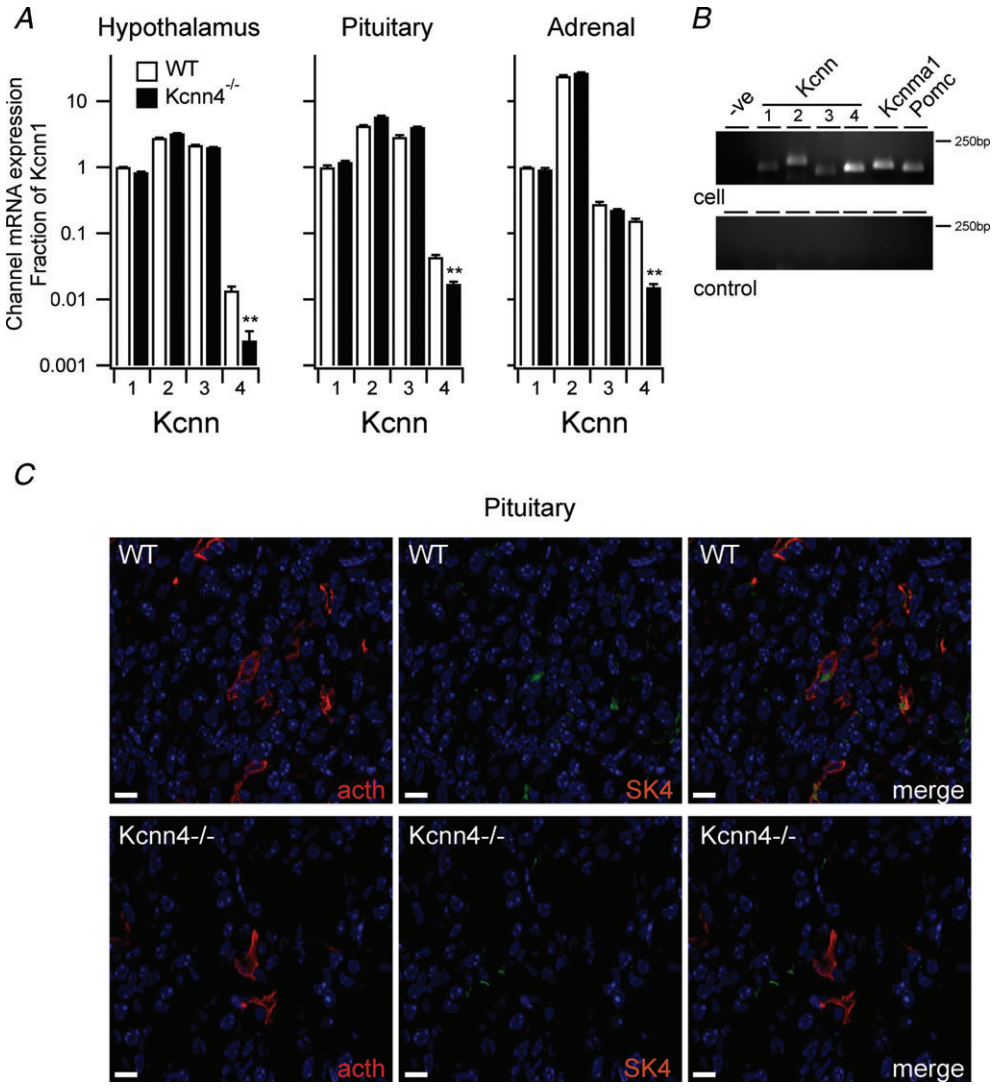

Figure 10. Expression of SK4 in HPA axis and anterior pituitary corticotrophs
A, mRNA expression encoding for SK4 channels (Kcnn4) and the related small conductance calcium-activated potassium channels SK1–3 (Kcnn1 to 3) determined by qRT-PCR in hypothalamus, anterior pituitary and adrenal gland from wild-type (WT, open bar) and Kcnn4 knockout mice (Kcnn4$^{-/-}$, filled bar). For each tissue, data are expressed as a fraction of the mRNA expression for Kcnn1. Data are means ± SEM, $n = 7$. $^{**}P < 0.01$, Kruskal–Wallis with *post hoc* Dunnett's test compared to WT. *B*, PCR amplicons from end-point single cell RT-PCR analysis from a fluorescently labelled corticotroph (cell) and negative sampling control (control) using primers to amplify Kcnn1–4, Kcnma1 and Pomc mRNA. –ve indicates PCR control. *C*, representative fluorescence images of anterior pituitary sections from wild-type (WT, top panels) and SK4 knockout (Kcnn4$^{-/-}$, bottom panels) mice probed for ACTH (left panels, red), and SK4 (middle panels, green) immunoreactivity with merged images shown at the right. Scale bars are 10 μm.

mRNA encoding for SK4 channels, as well as mRNA encoding small (SK1–3) and large (BK) conductance calcium-activated potassium channels, were detectable in cellular aspirates from single, fluorescently labelled corticotrophs positive for POMC mRNA (Fig. 10*B*). To examine whether SK4 protein is detectable in corticotrophs of the anterior pituitary we undertook dual-labelling immunohistochemistry in sections of the murine pituitary gland. Low levels of SK4 expression were detectable in wild-type animals (Fig. 10*C*), and quantitative distribution analysis demonstrated that $87.5 \pm 9.3\%$ of all ACTH-positive cells also expressed SK4 immunoreactivity. Conversely, $83.5 \pm 7.7\%$ of SK4-positive pituitary cells were also ACTH-positive. Therefore, the majority of SK4 expression in the anterior pituitary occurs in corticotrophs. While robust ACTH immunoreactivity was still evident, only non-specific background staining was detectable for SK4 in Kcnn4$^{-/-}$ mice.

To address whether global deletion of Kcnn4 function may result in additional stress hyperresponsiveness through enhanced excitation at the level of the hypothalamus we first examined the mRNA expression levels of the two early-immediate genes (c-*fos* and *nurr*77) as markers of hypothalamic activation (Chan *et al.* 1993; Brunton *et al.* 2007) in WT and Kcnn4$^{-/-}$ mice under control and restraint stress conditions (Fig. 11*A*). Control levels of c-*fos* mRNA expresssion were not significantly different between genotypes. Restraint stress induced a robust increase in c-*fos* mRNA expression in WT and Kcnn4$^{-/-}$ mice, as expected. However the increase in expression was significantly enhanced in the knockout. For *nurr*77 there was a small but significant increase in basal mRNA expression in the Kcnn4$^{-/-}$ mice compared to WT, an effect that was also maintained under stress conditions (Fig. 11*A*). Kcnn4$^{-/-}$ mice also displayed a significant increase in expression of both CRH and AVP mRNA. Under basal conditions, CRH mRNA expression in Kcnn4$^{-/-}$ mice was 2-fold higher than WT basal, and similar to that observed after 30 min restraint in WT mice. CRH mRNA levels in Kcnn4$^{-/-}$ mice were further increased following restraint, suggesting that CRH mRNA expression was not maximal, but remained sensitive to stress inputs. For AVP mRNA expression, basal levels in Kcnn4$^{-/-}$ mice were again higher than in WT basal, and similar to those seen after restraint in WT. However, no further increase in AVP mRNA expression was observed following restraint in Kcnn4$^{-/-}$ mice. This suggests that either AVP mRNA levels are maximally stimulated under basal conditions, or that stress-induced regulation of AVP mRNA levels is attenuated in the Kcnn4$^{-/-}$ mice.

Although there was a small (<40%) increase in mineralocorticoid receptor (MR) mRNA expression (Fig. 11*A*) no significant changes in glucocorticoid receptor (GR) mRNA expression were observed between genotypes under control or stress conditions. This suggests that the stress-induced negative feedback circuitry is largely unaffected. Taken together, these data suggest that enhanced stress-induced activation of the hypothalamus, as well as elevated expression of the major ACTH secretagogues, CRH and AVP, may contribute to the stress hyperresponsiveness observed in the Kcnn4$^{-/-}$ mice.

We next asked whether additional mechanisms might contribute to the stress hyperresponsive phenotype at the level of the anterior pituitary. Kcnn4$^{-/-}$ mice displayed a significantly elevated expression of mRNA for the G-protein coupled receptors for AVP (AVPR1b) and CRH (CRHR1) respectively in the anterior pituitary. This suggests that increased CRH and AVP receptor density may, in part, contribute to the enhanced evoked ACTH output in Kcnn4$^{-/-}$ corticotrophs *in vivo* and *in vitro*. There was no significant difference in POMC mRNA expression between genotypes under basal conditions (Fig. 11*B*) although levels after stress were modestly increased in the Kcnn4$^{-/-}$ mice. As for the hypothalamus, a small (∼40%), but significant, increase in MR, but not GR, mRNA expression was observed. Whether such modest increases in MR abundance at hypothalamic and/or pituitary levels could contribute to stress hypersensitivity is not known.

Although the plasma CORT responses in Kcnn4$^{-/-}$ mice followed the changes in plasma ACTH, suggesting that adrenal function *per se* was not compromised, we examined whether significant changes in adrenal function may contribute to the stress hyperresponsive phenotype in the Kcnn4$^{-/-}$ mice (Fig. 11*C*). No significant changes in mRNA expression for the ACTH receptor, MR or GR were observed under control or stress conditions. Furthermore, no significant changes were observed in mRNA expression of the two major enzymes required for CORT biosynthesis in the adrenal gland: cytochrome P450 side chain cleaving enzyme (Cyp11a1) required for synthesis of pregnenolone from cholesterol, and 3-β-hydroxysteroid dehydrogenase/Δ-5–4 isomerase (Hsd3b2), required for conversion of pregnenolone to progesterone.

Taken together these data suggest that SK4 channels may contribute to HPA axis function at multiple levels, including the anterior pituitary corticotroph and hypothalamic neural circuitry.

Discussion

In this paper we present a highly specific and efficient approach for labelling murine anterior pituitary corticotrophs using a lentiviral driven fluorescent eYFP reporter. This has allowed the first systematic analysis of the spontaneous and stimulated electrophysiological properties of murine corticotrophs. Importantly, our

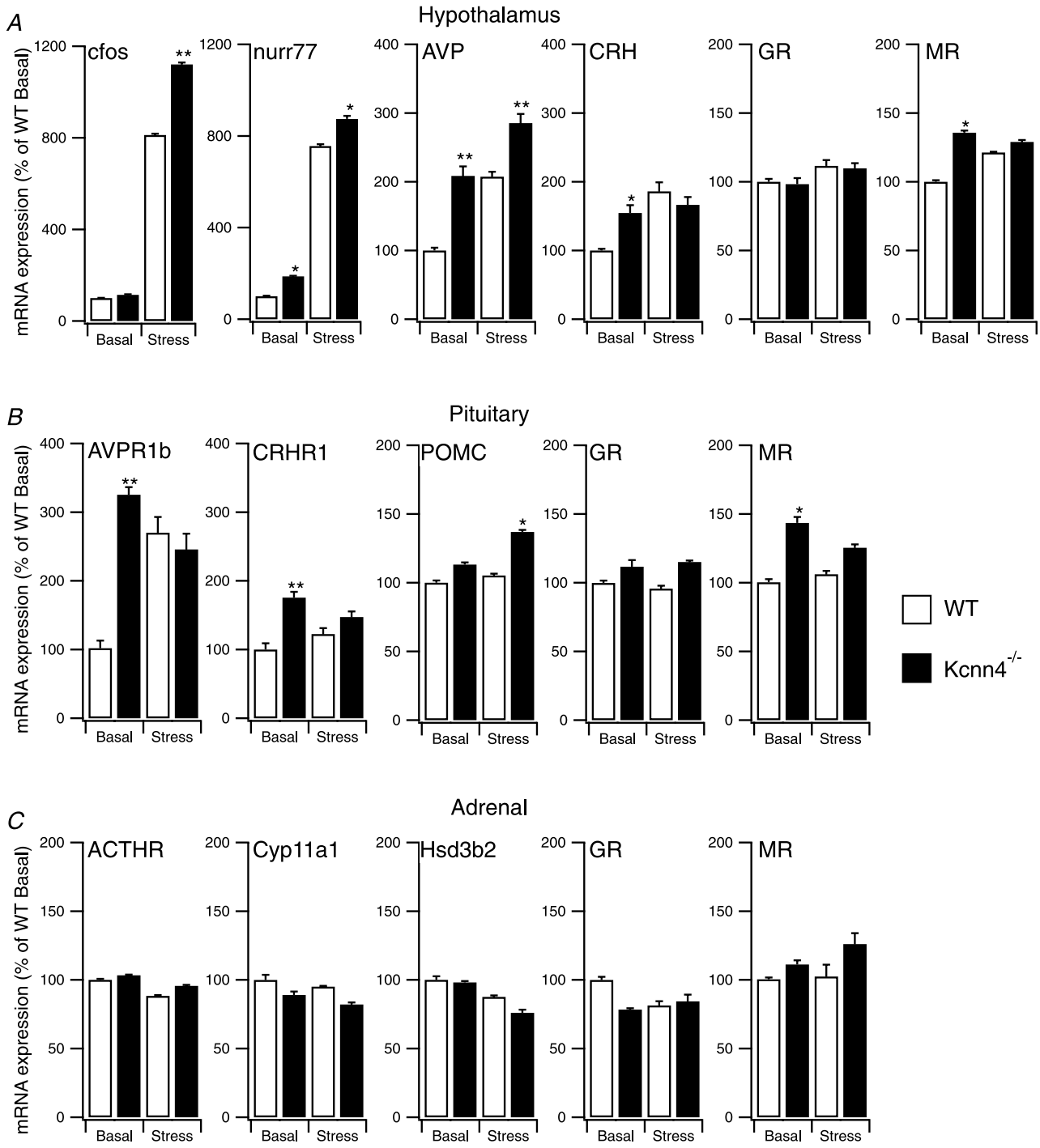

Figure 11. Enhanced hypothalamic activation and increased CRH and AVP mRNA expression in Kcnn4$^{-/-}$ mice

A–*C*, mRNA expression of selected genes in hypothalamus (*A*), anterior pituitary (*B*) or adrenal gland (*C*). mRNA expression was determined by qRT-PCR, under resting conditions (Basal) and following 30 min of restraint stress (Stress), from wild-type (WT, open bar) and SK4 knockout mice (Kcnn4$^{-/-}$, filled bar). mRNA expression was determined for: the markers of neural activation c-*fos* and *nurr*77; the peptides CRH and AVP; glucocorticoid (GR) and mineralocorticoid (MR) receptors; the G-protein coupled receptors for AVP (AVPR1b) and CRH (CRHR1); proopioiomelanocortin (POMC); the ACTH receptor (ACTHR); and the two major rate limiting enzymes in the corticosterone biosynthesis pathway, cytochrome P450 side chain cleaving enzyme (Cyp11a1) and 3-β-hydroxysteroid dehydrogenase/Δ-5–4 isomerase (Hsd3b2). Data are expressed as a percentage of the respective WT basal value (100%) with means ± SEM, $n = 7$. *$P < 0.05$ and **$P < 0.01$, Kruskal–Wallis with *post hoc* Dunnett's test compared to respective WT basal or WT restraint stress mRNA expression.

studies reveal a novel role for intermediate conductance calcium-activated potassium (SK4) channels in corticotroph function and demonstrate that mice deficient for this channel display stress hyperresponsiveness, at least in part, due to exaggerated CRH/AVP-evoked ACTH release from corticotrophs.

Specific and high efficiency labelling of murine corticotrophs

By exploiting lentiviral-mediated transduction of murine corticotrophs using eYFP driven by a minimal POMC promoter we have been able to label anterior pituitary corticotroph cells with >95% efficiency and >99% specificity without compromising corticotroph function. Perforated patch clamp recordings of labelled cells revealed that the large majority of murine corticotrophs tested displayed spontaneous electrical activity, and that frequency and patterns of spontaneous action potentials varied widely between cells. In the majority of cells, spontaneous activity was dominated by single action potential spikes. Single spikes displayed a bimodal distribution in the amplitude of the after-hyperpolarisation (AHP) following the spike. We thus classified spikes as either type A or type B where type A spikes had the larger AHP amplitude (>25 mV). In individual cells, single spikes rarely transitioned between the type A and type B phenotype. However, cells spontaneously transitioned from type A or type B spikes to more complex 'pseudo-plateau bursting modes' during recordings, reflecting spontaneous fluctuations in depolarising and hyperpolarising conductances with time. A major challenge for the future will be to determine whether such heterogeneity in corticotroph spontaneous activity exists in the intact pituitary and, more importantly, understand the relationship between different action potential firing patterns and the control of both 'basal' and stimulated ACTH secretion.

Importantly, metabolically intact murine corticotrophs used in our studies were spontaneously active and responded to physiological (low or subnanomolar) concentrations of CRH and AVP with a rapid and sustained increase in action potential firing and an associated depolarisation of the membrane potential. The vast majority of previous studies in various models have typically used CRH and/or AVP concentrations several orders of magnitude (typically 10–100 nM CRH, 20–100 nM AVP) higher than physiological levels in the portal circulation (Gibbs & Vale, 1982; Sheward & Fink, 1991).

A number of different transgenic mouse lines expressing fluorescent proteins under control of the POMC promoter, including that used in aspects of our study (Pinto *et al.* 2004), have very recently begun to be exploited to understand corticotroph regulation (Lee *et al.* 2011) and development (Budry *et al.* 2011) although the electrical or secretory properties of corticotrophs from these transgenic models have not been explored. Our lentiviral-labelling approach should complement these models and, in addition, allow rapid genetic manipulation (e.g. knockdown and/or overexpression of multiple genes) as well as interrogation of corticotrophs in other species in which transgenic models are not readily available.

A background sodium conductance controls resting membrane potential

In accordance with most previous studies in corticotrophs, inhibition of low micromolar tetrodotoxin (TTX)-sensitive voltage-dependent sodium channels had no consistent effect on generation of spontaneous action potentials (Surprenant, 1982; Kuryshev *et al.* 1997). However, replacement of extracellular Na^+ ions with the large organic cation $NMDG^+$ resulted in a robust hyperpolarisation of the cell membrane potential and cessation of spontaneous action potentials. Furthermore, a background Na^+ conductance was recorded at the potassium reversal potential, suggesting that a background Na^+ conductance is import in setting the resting membrane potential of murine corticotrophs. CRH has been reported to activate a non-selective cation current in human corticotrophs derived from both an ACTH-secreting adenoma as well as from non-adenoma tissue (Takano *et al.* 1996). This conductance was blocked by the large cation tetramethylammonium (TMA^+) but supported by lithium ions. These are characteristics shared with cAMP-activated non-selective cation conductances that also maintain a depolarised resting membrane potential of many other pituitary cell types, from both rat and mouse (Tomic *et al.* 2011). Although the molecular identity of this conductance has not been determined, recent pharmacological data support the role for members of the canonical transient receptor potential (TrpC) family of sodium and calcium permeable ion channels (Tomic *et al.* 2011). However, in human corticotrophs derived from patients with Cushing's disease (Mollard *et al.* 1987), and in the murine AtT20 corticotroph cell line (Surprenant, 1982), replacement of sodium with large organic blockers is reported to have no significant effect on resting membrane potential or electrical excitability. Whether murine corticotrophs represent a closer model to normal human corticotrophs, or whether these differences might result from distinct recording or isolation approaches, or perhaps differences in sex of corticotrophs analysed remains to be examined.

Murine and rat corticotrophs appear to differ in the contribution of inwardly rectifying potassium channels to the control of spontaneous electrical activity. While

we observed robust Ba^{2+}-sensitive inwardly rectifying conductances in female murine corticotrophs used in these studies, inhibition of these conductances with Ba^{2+} had no significant effects on spontaneous activity, unlike the effects reported in male rat corticotrophs (Kuryshev *et al.* 1997). For example, in male rat corticotrophs 100 μM Ba^{2+} depolarised the membrane potential by ∼6 mV from a mean resting membrane potential ∼−60 mV (Kuryshev *et al.* 1997). Our modelling studies suggest that the inwardly rectifying potassium conductance and non-selective sodium conductance act antagonistically to control action potential firing. The observed differences in rat *vs.* murine corticotrophs may reflect the more depolarised resting potential of the murine corticotrophs and/or differences in the relative expression or rectification properties of these channels between the two species, or sexes, of corticotroph.

Intermediate conductance calcium activated channels control corticotroph function *in vivo* and *in vitro*

Surprisingly, a large component of the outward potassium conductance of murine corticotrophs was mediated by a TRAM-34- and clotrimazole-sensitive conductance, indicative of the intermediate calcium activated potassium (SK4) channel encoded by the Kcnn4 gene. Although clotrimazole has been reported to regulate potassium conductances in other anterior pituitary cells (Wu *et al.* 1999), clotrimazole may inhibit a variety of channels. At the concentrations used here, TRAM-34 is reputed to be highly selective for SK4 channels (Wulff *et al.* 2000, 2007) (although one report has suggested effects on other conductances; Schilling & Eder, 2007). Kcnn4 mRNA was expressed at low levels relative to other Kcnn1–3 genes encoding the small conductance calcium-activated potassium channels in the anterior pituitary. However, we could detect SK4 protein expression co-localised with ACTH positive cells in the murine anterior pituitary gland. Inhibition of SK4 channels with TRAM-34 resulted in an increased frequency of action potentials in corticotrophs, although this was not associated with a significant depolarisation in resting membrane potential of the cell like that routinely observed with CRH/AVP. TRAM-34 potentiated CRH/AVP-stimulated ACTH secretion *in vitro*, and genetic deletion of functional SK4 channels resulted in enhanced stress-evoked plasma ACTH levels *in vivo*. Taken together, these data suggest that CRH/AVP does not stimulate ACTH release through inhibition of SK4 channels *per se*, even though SK4 channels are regulated for example by reversible protein phosphorylation (Gerlach *et al.* 2000). In humans, the SK4 channel inhibitor clotrimazole is widely reported to elevate plasma cortisol levels (Wojtulewski *et al.* 1980), although this may result in part from the effects of clotrimazole on cytochrome P450 enzymes. SK4 inhibitors are being developed as treatments for a range of disorders, including as potent immunosuppressants (Wulff *et al.* 2007). Clearly, if SK4 channels also play a role in controlling human corticotroph function, parallel changes in HPA-axis reactivity must be considered. Speculatively, concurrently elevated cortisol levels could contribute to the immunosuppressant effects of the drugs.

The above data clearly point to a significant role of SK4 channels in controlling corticotroph function; however we also observed changes in stress-induced hypothalamic excitability and drive. In these studies, we used restraint stress as a mixed physical and psychological stressor that activates multiple higher brain centres (Pacak & Palkovits, 2001) ultimately converging on the CRH and/or AVP expressing neurones in the paraventricular nucleus (PVN) of the hypothalamus. To examine whether the stress hyperresponsiveness of the $Kcnn4^{-/-}$ mice may also result from changes at the hypothalamic level, we examined mRNA expression for the immediate early genes c-*fos* and *nurr*77, markers for enhanced hypothalamic neuronal activation (Chan *et al.* 1993; Brunton *et al.* 2007). Restraint stress-induced c-*fos* mRNA and *nurr*77 mRNA expression were elevated in the $Kcnn4^{-/-}$ mice compared to WT controls. In addition, CRH and AVP mRNA expression in the hypothalamus were significantly elevated in $Kcnn4^{-/-}$ mice. If these translate to increases in CRH and AVP peptide content and release, they should result in an enhanced drive to the anterior pituitary corticotroph. We also observed a significant increase in CRH and AVP receptor mRNA expression in the anterior pituitary of $Kcnn4^{-/-}$ mice. POMC mRNA expression did not differ from control mice. Taken together, these data suggest that increased hypothalamic drive, as well as increased corticotroph sensitivity to CRH and AVP, may also contribute to the stress hyperresponsiveness observed in $Kcnn4^{-/-}$ mice. The enhanced activation of hypothalamic PVN CRH and AVP neurones may result from either changes in intrinsic excitability of the neurones *per se* or through changes to the afferent inputs. Intriguingly, mice deficient for BK channels show a decrease in hypothalamic CRH mRNA expression, without significant effects on *nurr*77 expression in PVN neurones. This suggests that large- and intermediate-conductance calcium activated potassium channels exert opposite effects on hypothalamic PVN function (Brunton *et al.* 2007).

The increased hypothalamic drive observed in the $Kcnn4^{-/-}$ mice might result from deletion of SK4 channels from hypothalamic PVN neurones, or their inputs, *per se*. However, the HPA axis is controlled by complex feed-forward as well as feedback mechanisms operating at multiple levels of the axis (Sapolsky *et al.* 2000). Thus, the changes in the hypothalamus could potentially be secondary, positive feedforward responses to elevations in ACTH and CORT output resulting from SK4 channel loss

from pituitary corticotrophs. In support of this, Kcnn4 mRNA in the hypothalamus (as well as whole brain) is expressed at very low levels (at least an order of magnitude lower) compared to other calcium-activated potassium channels. Moreover, as SK4 channels play a role in a wide variety of physiological processes in the CNS and in the periphery, ranging from control of T-cell and microglial activation, cell proliferation, to vasodilatation and epithelial ion transport (Kaushal *et al.* 2007; Wulff *et al.* 2007; Köhler & Ruth, 2010), a global deletion of Kcnn4 may affect other homeostatic mechanisms that influence HPA axis function and compromise allostasis (McEwen & Wingfield, 2003).

In conclusion, we have exploited a high efficiency lentiviral-mediated transduction system to allow the routine identification and first systematic analysis of the electrophysiological properties of murine corticotrophs. Our data reveal a novel role for intermediate conductance calcium-activated potassium (SK4) channels in controlling corticotroph excitability and ACTH secretion *in vitro* and *in vivo*. Furthermore, our data also suggest that SK4 channels may play additional roles in controlling stress axis function through the control of hypothalamic PVN neuronal excitability and drive.

References

Antoni FA (1986). Hypothalamic control of adrenocorticotropin secretion: advances since the discovery of 41-residue corticotropin-releasing factor. *Endocr Rev* **7**, 351–378.

Bers DM, Patton CW & Nuccitelli R (1994). A practical guide to the preparation of Ca^{2+} buffers. *Methods Cell Biol* **40**, 3–29.

Brunton PJ, Sausbier M, Wietzorrek G, Sausbier U, Knaus H-G, Russell JA, Ruth P & Shipston MJ (2007). Hypothalamic-pituitary-adrenal axis hyporesponsiveness to restraint stress in mice deficient for large-conductance calcium- and voltage-activated potassium (BK) channels. *Endocrinology* **148**, 5496–5506.

Budry L, Lafont C, el Yandouzi T, Chauvet N, Conejero G, Drouin J & Mollard P (2011) Related pituitary cell lineages develop into interdigitted 3D cell networks. *Proc Natl Acad Sci U S A* 108, 12515–12520

Bustin SA, Benes V, Garson JA, Hellemans J, Huggett J, Kubista M, Mueller R, Nolan T, Pfaffl MW, Shipley GL, Vandesompele J & Wittwer CT (2009). The MIQE guidelines: minimum information for publication of quantitative real-time PCR experiments. *Clin Chem* **55**, 611–622.

Chan RKW, Brown ER, Ericsson A, Kovacs KJ & Sawchenko PE (1993). A comparison of 2 immediate-early genes, C-Fos and Ngfi-B, as markers for functional activation in stress-related neuroendocrine circuitry. *J Neurosci* **13**, 5126–5138.

Childs GV, Marchetti C & Brown AM (1987). Involvement of sodium channels and two types of calcium channels in the regulation of adrenocorticotropin release. *Endocrinology* **120**, 2059–2069.

Dallman MF, Akana SF, Cascio CS, Darlington DN, Jacobson L & Levin N (1987). Regulation of ACTH secretion: variations on a theme of B. *Rec Prog Hormo Res* **43**, 113–173.

Gerlach AC, Gangopadhyay NN & Devor DC (2000). Kinase-dependent regulation of the intermediate conductance, calcium-dependent potassium channel, hIK1. *J Biol Chem* **275**, 585–598.

Gibbs DM & Vale W (1982). Presence of corticotropin releasing factor-like immunoreactivity in hypophysial portal blood. *Endocrinology* **111**, 1418–1420.

Hammer GD, Fairchild-Huntress V & Low MJ (1990). Pituitary-specific and hormonally regulated gene expression directed by the rat proopiomelanocortin promoter in transgenic mice. *Mol Endocrinol* **4**, 1689–1697.

Hodgkinson SC, Allolio B, Landon J & Lowry PJ (1984). Development of a non-extracted 2-site immunoradiometric assay for corticotropin utilizing extreme amino-terminally and carboxy-terminally directed antibodies. *Biochem J* **218**, 703–711.

Kaushal V, Koeberle PD, Wang Y & Schlichter LC (2007). The Ca^{2+}-activated K^+ channel KCNN4/KCa3.1 contributes to microglia activation and nitric oxide-dependent neurodegeneration. *J Neurosci* **27**, 234–244.

Keith LD, Winslow JR & Reynolds RW (1978). A general procedure for estimation of corticosteroid response in individual rats. *Steroids* **31**, 523–531.

Köhler R & Ruth P (2010). Endothelial dysfunction and blood pressure alterations in K^+-channel transgenic mice. *Pflugers Arch* ***459****, 969–976.*

Kuryshev YA, Haak L, Childs GV & Ritchie AK (1997). Corticotropin releasing hormone inhibits an inwardly rectifying potassium current in rat corticotropes. *J Physiol* **502**, 265–279.

LeBeau AP, Robson AB, McKinnon AE, Donald RA & Sneyd J (1997). Generation of action potentials in a mathematical model of corticotrophs. *Biophys J* **73**, 1263–1275.

Lee AK, Smart JL, Rubinstein M, Low MJ & Tse A (2011). Reciprocal regulation of TREK-1 channels by arachidonic acid and CRH in mouse corticotropes. *Endocrinology* **152**, 1901–1910.

Lee AK & Tse A (1997). Mechanism underlying corticotropin-releasing hormone (CRH) triggered cytosolic Ca^{2+} rise in identified rat corticotrophs. *J Physiol* **504**, 367–378.

Livak KJ & Schmittgen TD (2001). Analysis of relative gene expression data using real-time quantitative PCR and the $2^{-\Delta\Delta CT}$ method. *Methods* **25**, 402–408.

McEwen BS & Wingfield JC (2003). The concept of allostasis in biology and biomedicine. *Horm Behav* **43**, 2–15.

Mollard P, Vacher P, Guerin J, Rogawski MA & Dufy B (1987). Electrical properties of cultured human adrenocorticotropin-secreting adenoma cells: effects of high K^+, corticotropin-releasing factor, and angiotensin II. *Endocrinology* **121**, 395–405.

Pacak K & Palkovits M (2001). Stressor specificity of central neuroendocrine responses: Implications for stress-related disorders. *Endocr Rev* **22**, 502–548.

Pennington AJ, Kelly JS & Antoni FA (1994). Selective enhancement of an A type potassium current by dexamethasone in a corticotroph cell line. *J Neuroendocrinol* **6**, 305–315.

Pinto S, Roseberry AG, Liu H, Diano S, Shanabrough M, Cai X, Friedman JM & Horvath TL (2004). Rapid rewiring of arcuate nucleus feeding circuits by leptin. *Science* **304**, 110–115.

Ritchie AK, Kuryshev YA & Childs GV (1996). Corticotropin-releasing hormone and calcium signaling in corticotropes. *Trends Endocrinol Metab* **7**, 365–369.

Sapolsky RM, Romero LM & Munck AU (2000). How do glucocorticoids influence stress responses? Integrating permissive, suppressive, stimulatory and preparative actions. *Endocr Rev* **21**, 55–89

Sausbier M, Matos JE, Sausbier U, Beranek G, Arntz C, Neuhuber W, Ruth P & Leipziger J (2006). Distal colonic K^+ secretion occurs via BK channels. *J Am Soc Nephrol* **17**, 1275–1282.

Schilling T & Eder C (2007). TRAM-34 inhibits nonselective cation channels. *Pflugers Arch* **454**, 559–563.

Sheward WJ & Fink G (1991). Effects of corticosterone on the secretion of corticotrophin-releasing factor, arginine vasopressin and oxytocin into hypophysial portal blood in long-term hypophysectomized rats. *J Endocrinol* **129**, 91–98.

Shipston MJ, Kelly JS & Antoni FA (1996). Glucocorticoids block protein kinase a inhibition of calcium-activated potassium channels. *J Biol Chem* **271**, 9197–9200.

Shorten PR, Robson AB, McKinnon AE & Wall DJ (2000). CRH-induced electrical activity and calcium signalling in pituitary corticotrophs. *J Theor Biol* **206**, 395–405.

Simasko SM (1994). A background sodium conductance is necessary for spontaneous depolarizations in rat pituitary cell line GH3. *Am J Physiol Cell Physiol* **266**, C709–C719.

Stojilkovic SS, Tabak J & Bertram R (2010). Ion channels and signaling in the pituitary gland. *Endocr Rev* **31**, 845–915.

Surprenant A (1982). Correlation between electrical activity and ACTH/β-endorphin secretion in mouse pituitary tumor cells. *J Cell Biol* **95**, 559–566.

Tabak J, Toporikova N, Freeman ME & Bertram R (2007). Low dose of dopamine may stimulate prolactin secretion by increasing fast potassium currents. *J Comput Neurosci* **22**, 211–222.

Takano K, Yasufuku-Takano J, Teramoto A & Fujita T (1996). Corticotropin-releasing hormone excites adrenocorticotropin-secreting human pituitary adenoma cells by activating a nonselective cation current. *J Clin Invest* **98**, 2033–2041.

Tomic M, Kucka M, Kretshmannova K, Li S, Nesterova M, Stratakis CA & Stojilkovic SS (2011). Role of non-selective cation channels in spontaneous and protein kinase A stimulated calcium signalling in pituitary cells. *Am J Physiol Endocrinol Metab* **301**, E370–379.

Tsaneva-Atanasova K, Sherman A, van Goor F & Stojilkovic SS (2007). Mechanism of spontaneous and receptor-controlled electrical activity in pituitary somatotrophs: experiments and theory. *J Neurophysiol* **98**, 131–144.

Tse A & Lee AK (1998). Arginine vasopressin triggers intracellular calcium release, a calcium-activated potassium current and exocytosis in identified rat corticotropes. *Endocrinology* **139**, 2246–2252.

Wojtulewski JA, Gow PJ, Walter J, Grahame R, Gibson T, Panayi GS & Mason J (1980). Clotrimazole in rheumatoid arthritis. *Ann Rheum Dis* **39**, 469–472.

Wu S-N, Li HF, Jan CR & Shen AY (1999). Inhibition of Ca^{2+}-activated K^+ current by clotrimazole in rat anterior pituitary GH3 cells. *Neuropharmacology* **38**, 979–989.

Wulff H, Kolski-Andreaco A, Sankaranarayanan A, Sabatier J-M & Shakkottai V (2007). Modulators of small- and intermediate-conductance calcium-activated potassium channels and their therapeutic indications. *Curr Med Chem* **14**, 1437–1457.

Wulff H, Miller MJ, Hansel W, Grissmer S, Cahalan MD & Chandy KG (2000). Design of a potent and selective inhibitor of the intermediate-conductance Ca^{2+}-activated K^+ channel, IKCa1: a potential immunosuppressant. *Proc Natl Acad Sci U S A* **97**, 8151–8156.

Yuan JS, Reed A, Chen F & Stewart CN (2006). Statistical analysis of real-time PCR data. *BMC Bioinformatics* **7**, 85.

Author contributions

Z.L. performed and analysed the majority of voltage- and current-clamp electrophysiological recordings; L.C. developed and validated the lentiviral pomc-eYFP reporters; H.McC., performed and analysed the qRT-PCR experiments; D.MacG., developed the corticotroph H-H model; D.McC. and J.K. performed and analysed electrophysiological recordings and pharmacological analysis; R.L. and M.J.S. conducted the *in vivo* stress experiments; S.R. and H.G.K performed the immuno-histochemical analysis of SK4 protein expression; M.S. and P.R. generated the Kcnn4 knockout mice; M.J.S. conceived the study, analysed and interpreted results and wrote the manuscript. All authors contributed to critical review and revision of the final manuscript.

Acknowledgements

We are grateful to Prof. M. Low for the generous gift of the minimal rat pomc promoter construct; Prof. J. Friedman for the Pomc-GFP expressing mice line; Prof. D. Trono for the psPAX2 packing plasmid, and to Dr Trudi Gillespie in the IMPACT imaging facility, Centre for Integrative Physiology for assistance in fluorescence and confocal microscopy. We thank Clement Kabagema-Bilan for technical assistance in animal maintenance and *in vivo* assays. The work was supported by a Wellcome Trust programme grant to H.G.K., P.R. and M.J.S. Z.L. was in receipt of a China PhD scholarship.